International Journal of Biological Macromolecules 322 (2025) 146405

Contents lists available at ScienceDirect

International Journal of Biological Macromolecules

journal homepage: www.elsevier.com/locate/ijbiomac

Humic acid aggregates with laccase and decreases the performance of the enzyme catalytic systems through various mechanisms

João Lopes [a,b,c], Dorinda Marques-da-Silva [a,b,c], Cláudia Peralta [d], Joaquim Rui Rodrigues [a,b,c], Daniela Vaz [b,c,d,e], Ricardo Lagoa [a,b,c,*]

[a] School of Technology and Management, Polytechnic Institute of Leiria, Morro do Lena-Alto do Vieiro, 2411-901 Leiria, Portugal
[b] Laboratory of Separation and Reaction Engineering-Laboratory of Catalysis and Materials (LSRE-LCM), Polytechnic Institute of Leiria, 2411-901 Leiria, Portugal
[c] Associate Laboratory in Chemical Engineering (ALiCE), Faculty of Engineering, University of Porto, Rua Dr. Roberto Frias, 4200-465 Porto, Portugal
[d] Coimbra Chemistry Centre (CQC), Institute of Molecular Sciences, Chemistry Department, University of Coimbra, 3004-535 Coimbra, Portugal
[e] School of Health Sciences, Polytechnic Institute of Leiria, 2411-901 Leiria, Portugal

ARTICLE INFO

Keywords:
Biocatalysis
Copper oxidases
Polycyclic aromatic hydrocarbons

ABSTRACT

Laccases are among the best-rated enzymes for industrial and environmental applications, yet their use in bioremediation is limited by interference from environmental components like humic acid (HA). This study evaluated HA impact on the oxidation of 2,2′-azino-bis-(3-ethylbenzothiazoline-6-sulphonate (ABTS) and two model pollutants — anthracene and methyl orange — by laccase(−mediator) systems. HA consistently diminished conversion rates, with EC50 values between 5 and 51 mg/L suggesting diverse inhibitory mechanisms. We investigated potential mechanisms including substrate sequestration, radical quenching, and chelation of laccase coppers by HA. Incubations with free and immobilized HA showed that adsorption can impede anthracene degradation, at least at high concentrations, but not methyl orange. Using chemically generated ABTS radical and azide-blocked enzyme, it was demonstrated that HA scavenges free radicals produced by laccase, though this alone did not fully explain the observed interference with catalysis. Further assays with metal chelator and added copper or calcium ruled out HA binding to the laccase metal centers. Instead, data from molecular docking, fluorescence, light scattering, and microscopy revealed that HA forms micrometer-scale aggregates with laccase that encapsulate the enzyme. This newly identified mechanism likely applies broadly to laccase-based systems and must be considered in applications involving aqueous media containing humic substances.

1. Introduction

Laccases are among the enzymes capturing more attention regarding novel biocatalytic industrial processes and environmental remediation. Participating in the decomposition of lignin in nature, they were initially studied for the pulp and paper industry, but the applications span from textile dye bleaching to organic synthesis and production of novel materials [1–3].

Laccases (EC 1.10.3.2) are multi copper oxidases that catalyze the reduction of molecular oxygen to water, with the concomitant monoelectronic oxidation of the substrate to a corresponding radical [1,2,4,5]. A range of phenols and aromatic amines can function as substrates of laccases, although limited by their redox potential. Laccases from fungi are the most potent, reaching reduction potentials close to 0.8 V, even so inferior to activated peroxidase enzymes [2,5,6]. However, laccases can still be applied to catalyze the transformation of compounds more difficult to oxidize by way of using redox mediators, like 2,2′-azino-bis(3-ethylbenzothiazoline-6-sulfonic acid) (ABTS). The mediators are directly oxidized by laccases at the catalytic pocket and diffuse to react with a non-substrate compound via a non-enzymatic reaction, thus allowing to employ laccases to target compounds not directly accessible. In fact, laccase-mediator systems are generally used in pulp delignification, indigo bleaching and bioremediation applications [1,2,7].

Catalytic systems based on laccases, alone or combined with a mediator, have been demonstrated to oxidize a diversity of environmental pollutants. The more successful and pursued applications are the degradation of textile dyes, halogenated pesticides and polycyclic

* Corresponding author at: School of Technology and Management, Polytechnic Institute of Leiria, Morro do Lena-Alto do Vieiro, 2411-901 Leiria, Portugal.
E-mail addresses: joao.m.lopes@ipleiria.pt (J. Lopes), dorinda.silva@ipleiria.pt (D. Marques-da-Silva), joaquim.rodrigues@ipleiria.pt (J.R. Rodrigues), dvaz@uc.pt (D. Vaz), ricardo.lagoa@ipleiria.pt (R. Lagoa).

https://doi.org/10.1016/j.ijbiomac.2025.146405
Received 16 May 2025; Received in revised form 13 July 2025; Accepted 28 July 2025
Available online 6 August 2025

aromatic hydrocarbons (PAHs) present in waters and soils [2,8–11]. In a pilot study with contaminated groundwater from gas station areas, a laccase-ABTS system provided extensive oxidation of anthracene, a prototypical PAH pollutant [9]. Despite the encouraging data, there are still difficulties to a wider use of laccase-based catalytic systems in environmental remediation, such as the possible interference of metal ions and organic matter present in the waters and soils [2,7–9,12]. Concerning the interference of organic matter like humic acid (HA), ambivalent effects have been reported on the performance of laccase and other oxidoreductase systems [7,11,13,14]. With horseradish peroxidase (HRP), the removal of 17α-ethinylestradiol was inhibited by river natural organic matter, but the primary mechanism of interference varied with the molecular weight fraction studied [14]. Also with HRP, HA showed to have both a facilitator and an inhibitor role on the catalyzed transformation of bisphenol A, depending on the concentration [13]. The transformation of the fungicide cyprodinil by effective laccase-mediator systems was also reduced by HA, but it was slightly increased when no mediators were added to the reaction media [7]. Very recently, laccase catalysis without mediators was inhibited by HA at concentrations as low as 10 mg/L [15].

HA is a fraction of natural organic matter that is soluble at alkaline pH but insoluble under acid conditions [16]. It is composed of amorphous, chemically complex and heterogeneous organic molecules, present in soluble and insoluble forms in waters and soils, and plays important roles in biogeochemical and pollutant transformation processes [17,18]. After the decomposition of plant and other forms of biomass, HA can chelate trace metal ions and reduce their toxicity or enhance the availability of iron for plant uptake, and has been linked to the formation of carcinogenic disinfection by-products during drinking water chlorination [16,19]. The humic molecules are formed by substituted aromatic and aliphatic hydrocarbon core structures, bearing weak acidic carboxylic- and phenolic-OH groups. The polyelectrolyte nature combined with substantially hydrophobic segments or sidechains afford HA the ability to interact with a diversity of inorganic and organic species [16,19–21].

The ability to bind hydrophobic pollutants is the basis for the most discussed mechanism of HA interference with enzymatic systems in environmental remediation [12,14,15]. HA and other forms of organic matter can sequester the substrate or target pollutants, reducing their availability for the degradation reaction and, consequently, decreasing the efficiency of the enzyme-catalyzed process. The polyelectrolyte nature and metal chelating properties of HA raise the hypothesis that it binds to the copper centers of laccase. In natural waters, process and laboratory aqueous media under mild acid or alkaline conditions, HA molecules carry electric negative charges due to the deprotonated carboxylic and phenolic groups [16,20]. Both of these groups have been implicated in the binding of free copper ions to HA, with bidentate carboxylic-Cu complexation granting the dominant contributions to stable metal chelation [19,20]. There are indications that specific laccase's copper ions are solvent-accessible or labile [2,4,22,23], and other metal chelating compounds inhibited laccase catalytic activities [2,24]. On this basis, the chelation of the critical copper ions at the laccase active site is a plausible mechanism of inhibition of the enzyme by HA. However, this hypothesis has not been experimentally assessed, and it is debated whether the metal chelators indeed bind or withdraw the ions from the enzyme [2].

Another potential interference mechanism is supported by the ability of HA to react with free radicals [13,18]. Laccase catalysis involves the generation of different reactive radical intermediates and products [1,2,10,13], and HA contains significant electron donating capacity that can scavenge or reduce back the enzyme-produced radicals, therefore opposing the catalyzed reaction [18]. The involvement of dissolved organic matter in cross-coupling reactions with triclosan was also pointed out as a cause of the decreased yield in triclosan oxidized products generated by soybean peroxidase in the presence of organic matter [25].

The aim of this work was to investigate the modulatory (inhibition or facilitation) effect of HA and the mechanisms by which it interferes with laccase catalytic systems. Typical reactional systems were employed, with the enzyme alone and mediated by ABTS, in the degradation of the model pollutants anthracene and the azo dye methyl orange (MO). The actual relevance of the hypothetical mechanisms above-mentioned were thoroughly investigated by using diverse approaches, and the formation of aggregating laccase-HA complexes was revealed for the first time.

2. Materials and methods

2.1. Reagents, laccase and humic acid

HA was obtained as sodium salt from Acros, Geel, Belgium (cat. no. 120861000), as well as anthraquinone (104930500) and copper (II) chloride (206345000). Anthracene, potassium hydrogen phthalate and sodium alginate were supplied by Sigma-Aldrich, St. Louis, MO, USA (cat. nos. A89200, 33325 and A2033). MO and calcium chloride were from Panreac, Barcelona, Spain (281432.1209 and 1023820500). Diammonium salt of ABTS was purchased from Alfa Aesar, Haverhill, MA, USA (cat. no. J65535), while sodium acetate and diethylenetriaminepentaacetic acid (DTPA) were from Merck, Darmstadt, Germany (106268 and D6518), and hexane from Fisher Chemical, Geel, Belgium (H/0355/17). All other chemical reagents were HPLC or analytical grade.

The laccase used was from the fungi *Trametes versicolor* and was obtained from Sigma-Aldrich (cat. no. 38429). All the studies with laccase in this work were carried out in 100 mM sodium acetate buffer pH 5.

Laccase stock solutions were prepared in distilled water containing glycerol (20 % *v*/v). The laccase activity was determined spectrophotometrically with ABTS as a substrate at 500 μM, with 1 μg/mL of the enzyme, in the acetate buffer pH 5, at 25 °C. ABTS oxidation was followed at 420 nm and one unit (U) of laccase activity was defined as the amount of enzyme that catalyzes the oxidation of 1 μmol of ABTS per min. The molar absorption coefficient (ε) of the ABTS radical was considered 3.6×10^4 M^{-1} cm^{-1} [26].

HA solutions were prepared as described in our previous work [27]. In brief, HA was dissolved in NaOH 100 mM and then centrifuged at 5533*g*, for 20 min, in a Heraeus Biofuge Stratos Centrifuge (Kendro Laboratory Products, Germany). Phthalate buffer at 0.5 M was added to the supernatant and the pH was adjusted to 4.5. The solution was centrifuged identically, and the supernatant HA solution was reserved. Blank solutions without HA were prepared in parallel, following the same procedure, using the same volumes of NaOH and buffer, but not dissolving the HA powder at the beginning. These HA-blank solutions thus contained all the buffer constituents present in the HA solutions and were employed as controls in the HA tests. Before use, the HA solutions were filtered through a 0.2 μm pore filter. The concentration of HA was determined by oven drying samples completely and subtracting the weight of equivalent dried blank solutions from the weight of the dried HA solutions. Throughout this work, 4 batches of HA solutions were prepared with concentrations between 6.90 and 7.88 g/L.

2.2. Assays of laccase-catalyzed degradation of anthracene

Anthracene was added to the pH 5 acetate buffer at an initial concentration of 1 mg/L (5.6 μM), as well as 100 μg/mL of laccase (85 mU/mL) and ABTS at 50 μM. The stock solutions of anthracene were prepared in acetonitrile, hence the reaction media contained a minor quantity of this solvent, up to 1 % (*v*/v). The effect of HA concentrations (5, 50, 100, 300 and 500 mg/L) was tested by adding different amounts of HA to the reaction media before triggering the reaction with laccase. Control assays were performed either in the absence of HA or absence of laccase. The reaction tubes were tightly sealed and incubated in the absence of light at 20 °C, for 24 h.

At the end of the incubation, hexane extracts of the reaction media were prepared for HPLC analysis of the remaining anthracene and reaction products formed [6]. The extraction method consisted in adding a total of 1 mL of hexane to the media, in two 500 μL runs, to 1 mL of the reaction media and stirring vigorously for 30 s in each run (protected from light). At the end of each run, the organic phases were collected and combined for posterior HPLC analysis. The efficiency of this method for the extraction of anthracene and anthraquinone from the sodium acetate buffer used in the enzymatic assays was close to 100 % (Table S.1 of Supplementary Material). Even when a very high concentration of HA was present (250 mg/L), anthracene recoveries superior to 85 % were observed.

The HPLC analysis followed existing methods from our laboratory [6,27]. Briefly, an Agilent 1100 system equipped with a reverse phase C18 column was operated with an acetonitrile:water (85:15) mobile phase at 1 mL/min and UV detection at 251 nm. The retention times of anthracene and anthraquinone were 6.7 min and 4.5 min, respectively. The linearity of the response to anthracene and anthraquinone concentrations was evaluated with calibration curves obtained with at least 5 standards between 0.0625 and 1.00 mg/L of anthracene and between 0.0125 and 1.00 mg/L of anthraquinone in hexane. The degree of anthracene conversion was calculated by comparing the areas of its chromatographic peaks from the degradation assays with those from the controls. The ratio of anthraquinone formed to anthracene degraded (mol/mol) was calculated from the respective peaks in the degradation and control assays' chromatograms, and considering calibration curves of each compound.

2.3. Assays of laccase-catalyzed decolorization of methyl orange

The study of MO degradation was carried out with laccase alone and the laccase-ABTS system. The assays were performed with 300 μg/mL (255 mU/mL) of laccase alone, or 100 μg/mL (85 mU/mL) in the presence of 50 μM ABTS for the laccase-ABTS system, to degrade 10 mg/L of MO at 25 °C. MO decolorization was monitored by the decrease in the absorbance of the reaction media at 477 nm (Genesys 10 UV–Vis spectrophotometer, Thermo Scientific, USA). After some minutes of incubation, HA was added in volumes corresponding to final concentrations of 1, 5, 15, 25, 50, 75 and 100 mg/L. HA inhibition was calculated by comparing the decolorization rates before and after the addition of HA to the reaction media. Control assays were carried out for all HA concentrations tested by adding equal volumes of HA-blank solution instead of HA solution.

2.4. Assays of laccase-catalyzed oxidation of ABTS

The oxidation of ABTS was also assayed in the above-indicated acetate buffer (pH 5) at 25 °C, using a concentration of laccase 1 μg/mL. The initial concentration of ABTS was 50 μM, and the formation of the one-electron oxidized ABTS radical was monitored at 420 nm [2].

For studying the inhibition by HA, the oxidation of ABTS was followed for some minutes and, then, small volumes of HA were added to the reaction media to reach final concentrations of 1, 5, 10, 25, 50, 75, 100, 150 and 350 mg/L. Control assays were carried out using the same reaction media, but adding equal volumes of the HA-blank solution instead of the HA solution. The HA inhibition was computed from the ABTS oxidation rate before and after the addition of HA or blank solution.

The same method of laccase-catalyzed ABTS oxidation was adopted for studying the effect of DTPA on the enzyme activity, as well as of copper (II) and calcium ions. The inhibition by DTPA was assayed by the addition of small volumes of stock solution to the reaction media to reach a final concentration of 0.01, 0.1, 0.2, 0.3, 0.4, 1, 3, 5 and 7 mM of DTPA. The effect of HA in DTPA-inhibited laccase was studied by monitoring the oxidation of ABTS for 25 min, then adding 0.4 mM of DTPA to the reaction media, keep following the ABTS oxidation for 5 min, and then adding 50 mg/L of HA to the reactional media. Similarly, the effect of copper (II) and calcium ions in HA inhibition was studied by following the oxidation of ABTS for 10 min, then adding small volumes of $CuCl_2$ or $CaCl_2$ to 1 mM in the reaction media, and afterwards HA to reach a final concentration of 50 mg/L.

2.5. Uptake of anthracene and methyl orange by humic acid in beads

Alginate beads encapsulating HA were prepared by adapting the calcium-induced alginate gelation method [28]. First, solutions of sodium alginate 2 % (*w/v*) were prepared in distilled water, by dissolution and with gentle agitation overnight. Then, HA was slowly added to the alginate solution to a final concentration of 0.5 % (w/v) and, afterwards, the mixture was dropped into a 150 mM $CaCl_2$ solution under stirring. The forming gel beads were kept in the calcium solution, with gentle agitation, for at least 8 h for complete gelation. Unloaded calcium alginate beads were prepared by the same method, except that no HA was added. After gelation, the beads were separated from the gelation solution and reserved. The gelation solutions were used to calculate the amount of HA not encapsulated in the beads (encapsulation efficiency) and, thereafter, calculate the HA content of the loaded beads. The spectra of the gelation solutions (from unloaded and HA-loaded beads) were registered between 200 a 600 nm and, by comparing to standard dilutions of HA, the amount of HA not encapsulated was obtained and values of encapsulation efficiency of approximately 70 % were calculated. The gel beads were dried in an oven at 35 °C, until constant mass (3 days), and the HA content of the HA-loaded dry beads was 18 mg/g.

The dried beads, with and without HA, were used to study the adsorption of anthracene and MO. The studies were performed with two adsorbent doses (2.1 and 6.9 mg of beads in 2.5 mL solutions) corresponding to two concentrations of HA in the media, 15 mg/L and 50 mg/L. The assay solutions initially contained 1 mg/L anthracene or 10 mg/L MO, in 100 mM sodium acetate buffer (pH 5). Control assays had anthracene or MO in the media, but no beads, and were incubated under the same conditions. Blank assays were also carried out in parallel with each type of the beads, but without the PAH or the dye, to assess the possible interference of any component released from the beads during the incubation. All assays run for 48 h with gentle agitation, and were stopped by separating the beads from the liquid phase. In the case of MO, the spectra of the solutions after the incubations were registered between 300 and 600 nm to measure the remaining dye in the liquid phase. The amount of MO adsorbed to the beads was calculated from the remaining MO in the solutions of Control assays (no beads) and the assays with the studied beads, considering a ε (at 466 nm) of 25,100 M^{-1} cm^{-1}. The adsorbed dye was calculated as μmol/g of beads. The adsorbed anthracene was calculated from the PAH desorbed from the beads collected at the end of the adsorption assays. For desorption, the beads were placed in 2.5 mL of methanol, with gentle agitation for 48 h. Afterwards, the anthracene was measured by HPLC using the method described above, and the adsorbed PAH calculated as mg/g of beads.

2.6. Scavenging of free radicals by humic acid

The ability of HA to react with radical intermediates or products of the laccase-catalyzed MO and ABTS oxidation reactions was investigated by different methods. For the MO reactional system, the decolorization assay with laccase alone described in Section 2.3 was adopted. Dye transformation was followed for 30 min and sodium azide at 0.2 mM was added to the reaction media to block the enzyme. After stabilization of the absorbance at 477 nm, HA was added at 75 and 150 mg/L. The monitoring of the absorbance changes allowed to follow the initial decolorization, the laccase blockade, and if HA had any detectable effect.

An identical approach was made for the ABTS reactional system. The oxidation assay described in Section 2.4 was adopted, but the concentration of ABTS was 500 μM to reach a higher concentration of the ABTS

radical reaction product, favoring the observation of HA scavenging of the radical. The laccase-catalyzed oxidation of ABTS was registered until the 420 nm absorbance reached approximately 0.5, corresponding to 14 μM of ABTS radical, then the enzyme was blocked (sodium azide 0.1 mM), and HA was added to the reaction media at 75 and 150 mg/L.

The reaction of HA with ABTS radical was also tested in a laccase-free system, using ABTS radical produced by persulfate oxidation of ABTS. Beforehand, ABTS radical was obtained by mixing 10 mL of 7 mM ABTS with 10 mL of 4.9 mM potassium persulfate and leaving the mixture in the dark, at room temperature, for 12–16 h [26]. In this proportion, persulfate is limiting and ABTS is not completely oxidized. The scavenging assays were then carried out with this chemically produced ABTS radical, also at approximately 14 μM in the acetate buffer, following the effect of HA 75 and 150 mg/L at 420 nm.

2.7. Molecular docking of humic acid to laccase

The docking simulations were performed with AutoDock4 [29] with the laccase PDB structures 1kya and 1gyc. The model 1kya was determined by X-ray diffraction at a resolution of 2.40 Å and contains four chains A to D, each complexed with 2,5-xylidine in the putative active site and having 499 amino acids [30]. The protein is similar to the laccase III reported by Mikuni and Morohoshi (1997), having just 4 amino acid residues different [31]. The model was edited in ChimeraX [32] to retain chain A only, add missing heavy atoms, remove water molecules except those coordinated to the copper ions, remove atoms with alternative locations, add hydrogen atoms and Gasteiger partial charges. The resulting model was then used in AutoDockTools (ADT) to remove non-polar hydrogens atoms and to assign AutoDock atom types. The model 1gyc was determined at a resolution of 1.90 Å, contains only one polypeptide chain and no binding molecule in the active site [5]. It is a Laccase II and shares 80 % identity with 1kya. To prepare the protein for docking, the orientation of Asn, Gln and His side chains were optimized with the Reduce software [33] and, then, the model was edited with ChimeraX and ADT as for 1kya.

The HA models were obtained from the work of Niederer and Goss (2007), who devised four models (M1 to M4) derived from ^{13}C NMR, elemental, and acidic function data, that were used to predict equilibrium partitioning of organic vapors between air and HA [34]. The 2D structures were drawn using Marvin JS (ChemAxon, http://www.chemaxon.com), which was also used to generate the corresponding 3D SMILES strings. These were then processed in ChimeraX to create 3D models with calculated Gasteiger atomic partial charges. Finally, ADT was used to prepare the models for docking by defining torsions, removing non-polar hydrogen atoms, and assigning AutoDock atom types – the 3D structures of the models are shown in Fig. S.1.

The blind docking simulations were carried out on a set of grids computed with Autogrid4 positioned in the center of the protein and extending 10 Å from the protein limits in each direction. For 1kya, the grid map measured 71.2 × 79.5 × 91.5 Å and for 1gyc, 87.8 × 78.0 × 80.2 Å. Default parameters were used, except for the Cu parameters, which were taken from Corona-Motolinia et al. [35]. The conformational search was carried out with Autodock using the Lamarckian genetic algorithm with default parameters, except for number of runs (500), number of generations (40000), population size (300) and number of energy evaluations ($2{,}5 \times 10^7$). The figures were generated with VMD [36]. The free energy of binding estimated by Autodock was decomposed into the contributions from two terms [37]: the electrostatics energy, and the van der Waals and hydrogen bonding terms reported together as an aggregated value (vdW + Hbond).

2.8. Quenching of laccase fluorescence

The fluorescence studies were carried out on purified laccase samples, made free of contaminants by dialysis (Thermo Scientific Slide-A-Lyzer cassette, membrane cutoff 10 kDa) against 100 mM sodium acetate buffer, pH 5, followed by freeze-drying for 24 h, at −50 °C, 150 mT (Kinetics, Eschau-Hobbach, Germany), and centrifugation for 5 min, at 4000 *g* (Labofuge200, Heraeus, Hanau, Germany).

Fluorescence experiments were performed on a Varian Cary Eclipse fluorescence spectrophotometer (Agilent Technologies, Santa Clara, USA) equipped with a thermostated cell. Intrinsic fluorescence emission spectra (300 to 400 nm) were obtained at controlled temperature (25 °C), using an excitation wavelength of 280 nm and slits of 5 nm. Final fluorescence spectra were obtained upon inner filter effect correction and baseline subtraction. Laccase samples (20 μg/mL) in acetate buffer, pH 5, were analyzed in the absence and presence of HA (10, 20, 30 and 50 mg/L).

2.9. Dynamic light scattering experiments

Dynamic light scattering (DLS) measurements were carried out by making use of a Malvern Zetasizer Nano ZSP operating with a He—Ne laser (Malvern Instruments, UK) with a wavelength of 633 nm and a scattering angle of 13°. Measurements were recorded at 25 °C and each measurement was the average of 10 runs. The experimental results were analyzed using the built-in software Zetasizer 7.12, considering the viscosity and refractive index of water at the measurement's temperature, and a refractive index of 1.45 for the scattering particles. Values of hydrodynamic radius (r, nm) were obtained considering the Stokes–Einstein equation for diffusion and using the relation between diffusion and the scattering vector obtained from the DLS measurements. Three measurements were performed for each sample. Solutions of HA (20 mg/L) were analyzed first in the absence and then in the presence of laccase (20 μg/mL). The measurements were collected after an equilibration period of 1 min of the solutions in the cuvette, and the results were plotted as intensity of distribution (%) of particles versus hydrodynamic radius (nm).

2.10. Microscopy experiments

For the microscopic observations, incubations were prepared with laccase at 20 μg/mL, 20 mg/L HA and 1 mM $CaCl_2$, in acetate buffer. The incubations included laccase alone, HA alone, HA with Ca^{2+} ions, laccase with HA, and laccase with HA and Ca^{2+}. At the end of 24 h incubations at 25 °C, 1 mL aliquots were taken and centrifuged at 28190 *g* for 20 min at 4 °C. After centrifugation, the supernatant was discarded and the pellet was resuspended in the same buffer. To reveal the presence of laccase, ABTS was added at a concentration of 500 μM and incubated for 30 min. Then, the samples were dropped on a microscopic slide and observed in an Olympus CX41RF microscope (Olympus, Philippines). Samples of HA with Ca^{2+} were also incubated with oxidized ABTS (ABTS radical) from a separate solution containing laccase that was blocked with 0.2 mM sodium azide before addition to the HA aggregates. Photographs were taken at 400× magnification and a slide with a micrometer scale was used as reference to dimensions.

2.11. Presentation of results and statistical analysis

All the assays were carried out at least in triplicate experiments for each condition. Figures were produced showing the results in the form of representative chromatograms or experimental traces or as plots of Mean ± standard error (SE) for each condition. The vertical error bars in plots represent SE. The significance of the differences between experimental conditions was analyzed using one-way analysis of variance, and statistically significant differences were identified when $p \leq 0.05$.

3. Results

3.1. Laccase-catalyzed degradation of anthracene and methyl orange

Laccase from the white-rot fungi *T. versicolor*, one of the most

common and best-regarded laccases for industrial and environmental applications [1,2,7–12,15,30], was employed in this work. In spite of having a redox potential higher than their bacterial counterparts, fungal laccases typically are not able to directly oxidize PAHs and can only slowly decolorize some azo dyes [2,8,38,39]. Nevertheless, these concerning pollutants can be targeted by laccases by way of redox mediators, with ABTS being one of the most successful options [2,9,10,38]. Our results with anthracene and MO, using the laccase alone and combined with ABTS, are in good accordance with the published data.

As illustrated by the results in Fig. S.2, laccase alone showed no significant capacity to degrade anthracene in 24 h incubations, but the co-presence of ABTS enabled the transformation of the PAH into at least 2 products or intermediates detected by HPLC analysis of the hexane extracts from the reaction media. Although the effect of ABTS could be noted with low μM levels, it was amplified by concentrations up to 50 μM (Fig. S.2.B). Hence, this mediator concentration was used in the following assays of HA inhibition. Based on the peak area, the main reaction product repeatedly observed in the chromatograms was 9,10-anthraquinone, as confirmed using a standard (Fig. S.2.A). Also in agreement with the published data [2,8], the quantity of anthraquinone measured was approximately half the quantity of anthracene transformed (ratio close to 0.5 mol/mol). This discrepancy is not due to incomplete extraction of anthraquinone from the reaction media (Table S.1), but, as discussed for different laccase- and peroxidase-based systems, an evidence of the complex route(s) of anthracene oxidation [2,8,40]. Anthraquinone is surely one of the more stable products, but anthrone, hydroxylated polycyclic intermediates or products, and ring cleavage species have been identified simultaneously in these reactional systems.

The laccase-catalyzed oxidation of MO at pH 5 was followed by the decolorization of dye solutions. Most azo dyes are toxic and refractory to conventional treatment processes [10]. As shown in Fig. S.3, laccase was able to transform MO, though ABTS greatly accelerated the rate of decolorization. Comparable to anthracene, MO transformation was promoted via an ABTS-mediated process in concentrations up to 50 μM. It should be noted that complete decolorization of the azo dyes is not expected, as the laccase-catalyzed reactions generate phenoxy radicals and carbocations, among other intermediates, preceding azo bond cleavage and formation of degradation products with smaller molecular weight but still retaining some coloration [10,38]. Nonetheless, the decolorization of MO offered an interesting method to investigate the effect of HA in both laccase (alone) catalysis and in a laccase-ABTS system.

3.2. Humic acid inhibition of laccase-catalyzed degradation of anthracene and methyl orange

The effect of HA was investigated in the different laccase (alone and mediated) systems. HA stock solutions were prepared by alkaline dissolution and adjusting the final pH to 4.5, along with HA-blank solutions, as described in Methods Section 2.1. Anthracene transformation catalyzed by the laccase-ABTS system was clearly inhibited when HA was present in the reaction media (Fig. 1). In the absence of HA, a 70 % conversion of the PAH could be reached in the assays with 50 μM ABTS (Figs. S1·B and 1.A). However, HA at concentrations above 50 mg/L caused a large decrease, more than 40 % inhibition, of the anthracene conversion (Fig. 1.B). The HA effect on anthracene degradation was observed in the HPLC chromatograms both by the smaller decrease of the anthracene peak and the lower production of reaction products (Fig. 1.A). The yield of anthraquinone, relative to anthracene converted, was found to be maintained close to 0.5 mol/mol through the whole interval of HA concentrations tested (inset in Fig. 1.B), suggesting that HA does not affect the path of reactions after anthracene oxidation by the laccase-ABTS system.

The inhibition data were fitted to the equation of a hyperbolic curve consistent with the binding model of a ligand to a single-site in the target:

$$\text{Inhibition} = \frac{I_{max} \times [HA]}{EC_{50} + [HA]} \quad (1)$$

where [HA] is the concentration of HA, I_{max} the maximal inhibition and EC_{50} is the half-maximal effect concentration of HA. All the inhibition results in this work fitted this model quite well, with correlation coefficients (R^2) above 0.95.

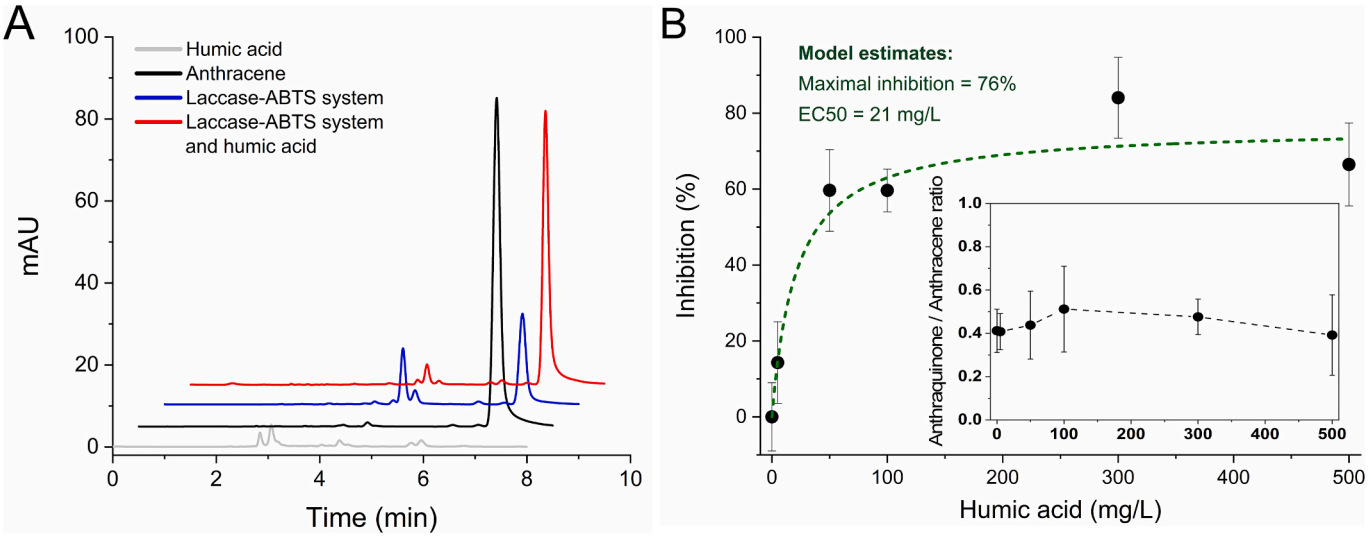

Fig. 1. Effect of humic acid on laccase-ABTS degradation of anthracene. (A) HPLC chromatograms of anthracene degradation by laccase-ABTS system, in the absence and in the presence of humic acid (500 mg/L). Assays were carried out with an initial concentration of anthracene 1 mg/L, laccase 100 μg/mL and ABTS 50 μM. After 24 h incubation, the reaction media was extracted with hexane and analyzed by HPLC. Chromatograms from anthracene and humic acid controls, incubated in the absence of enzyme, are also shown. The chromatograms are displaced on the vertical and horizontal axes for better observation. (B) Inhibition of laccase-ABTS degradation of anthracene by humic acid. Assays were carried out as in (A) and the inhibition was calculated from the degradation in the presence of humic acid compared to the respective control without humic acid. The anthracene degradation in the control assays was 70 ± 14 %. The line is the best non-linear regression fit of the data to Eq. (1) in the text, and the corresponding parameters are indicated (R^2 = 0.957). The inset plots the ratio of anthraquinone formed to anthracene degraded (mol/mol) measured in the presence of the different concentrations of humic acid.

For anthracene transformation, the value of EC_{50} calculated was 21 mg/L. Surprisingly, the maximal inhibition did not reach 100 %, not even when very high concentrations of HA were present in the reaction media (Fig. 1.B).

Fig. 2.A shows representative experimental traces from assays of the effect of HA on the decolorization of MO by laccase (alone). The rate of decolorization was small in this case as expected, but sizable in 10-min periods. When HA was added to the reaction media, a sudden increase in the absorbance of the solution was observed, because HA absorbs at the monitored wavelength. Then, 1–3 min after the addition, a steady rate of decolorization is reestablished, but smaller than that observed in the absence of HA. The blue experimental trace in Fig. 2.A allows to observe the inhibition caused by a first addition of HA that results in a concentration of 20 mg/L, and a subsequent addition of more HA to a final concentration of 100 mg/L in the reaction media. An equivalent experimental trace (in black) is also depicted corresponding to a control assay using the HA-blank solution, added in the same volumes as the HA stock solution in the test assay. The control assays with HA-blank solutions showed no significant inhibition of the laccase catalytic systems, indicating that the buffer constituents used in the preparation of the HA stock solutions had no major effect on laccase.

The rate of MO decolorization by the laccase-ABTS system was much faster, but also sensitive to the presence of HA. An experimental trace is depicted in Fig. S.3.A showing the inhibition of the laccase catalytic system mediated by ABTS 50 μM. The quantification of the HA inhibition of MO decolorization catalyzed by the two laccase catalytic systems revealed that the dependency on the HA concentration is very similar (Fig. 2.B). Both with the laccase alone and the ABTS-mediated system, a plateau of maximal inhibition close to 30 % was calculated, even lower than that observed for the anthracene degradation.

3.3. Humic acid inhibition of laccase-catalyzed oxidation of ABTS

The fact that HA inhibited MO decolorization catalyzed by laccase alone, similarly to the effect on the laccase-ABTS system, was a strong indicator that the driving mechanism of HA inhibition is not related to the mediator role. The primary mechanism(s) must be connected to some interaction of HA with the enzyme and/or with the substrates. Hence, we decided to assess the effect of HA in the direct oxidation of ABTS to ABTS radical catalyzed by laccase, a simple and defined reactional system. The production of ABTS radical in the reaction media is easily tracked at 420 nm and HA was found to also inhibit this reaction (Fig. 3). As depicted in the experimental traces of Fig. 3.A, the addition of HA to the reaction media causes an abrupt increase in absorbance (not detectable with low concentrations like 1 mg/L), for the same reason indicated for the MO assays. Afterwards, a biphasic effect of HA was observed: in the first minutes, the absorbance does not increase until, gradually, a steady rise of absorbance is reestablished. In the first phase, the absorbance change paused or even decreased with high concentrations of HA, e.g. 50 mg/L (Fig. 3.A), suggesting that HA is blocking the production of the ABTS radical and/or reducing it back. In any case, this effect was transient, and a stable oxidation rate was restored and maintained for a long time.

The quantification of the steady rates of absorbance increase evidenced the HA inhibition of the ABTS-oxidizing activity of laccase. With HA concentrations superior to 25 mg/L, the oxidation rates were significantly inferior to those measured in control assays with HA-blank solutions (Fig. 3.B). However, the inhibition did not reach 100 % despite the very high HA concentrations tested. The experimental data fitted the Eq. (1) with a perfectly acceptable R^2 of 0.991 (Fig. 3.B), but the existence of a plateau of maximal inhibition, as in the previously studied reactional systems, weakens the hypothesis that HA directly interacts with some critical component of laccase. Instead, the differences in the maximal inhibitions and EC_{50} values determined for the several reactional systems (Fig. 1.B, 2.B and 3.B) suggest that HA effects are dependent on the substrate or target pollutant.

3.4. Sequestration of anthracene and methyl orange by humic acid

A simple explanation for the HA interference with laccase-based systems is the sequestration of the substrates, or of the target compounds, limiting the observed catalytic activity of the enzyme. HA

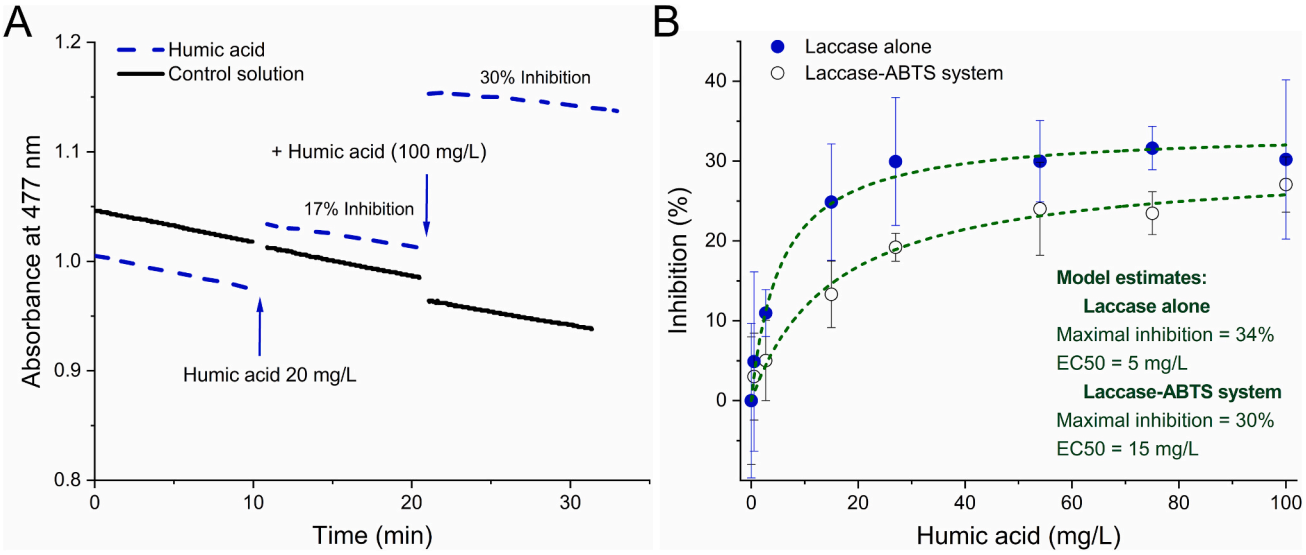

Fig. 2. Effect of humic acid on laccase-catalyzed decolorization of methyl orange. (A) Assays of methyl orange decolorization by laccase (alone). Small volumes of humic acid stock solution were added to the spectrophotometer cuvette to reach the final concentrations indicated. In the control assay, equivalent volumes of HA-blank solution (buffer without humic acid) were added to the cuvette. The humic acid-induced inhibition of the enzyme was calculated as % relative to the initial decolorization rate in the absence of humic acid.
(B) Humic acid-induced inhibition of methyl orange decolorization by the laccase alone and the laccase-ABTS system. The inhibition was calculated from the decolorization rates in the presence of humic acid compared to the corresponding control rate in the absence of humic acid. The control decolorization rates, in ΔAbs/Δt, of the laccase alone and the ABTS system were -0.003 ± 0.001 min^{-1} and -0.029 ± 0.005 min^{-1}, respectively. The lines are the best non-linear regression fits of the data to eq. (1) in the text, and the corresponding parameters are indicated ($R^2 = 0.996$ and 0.980).

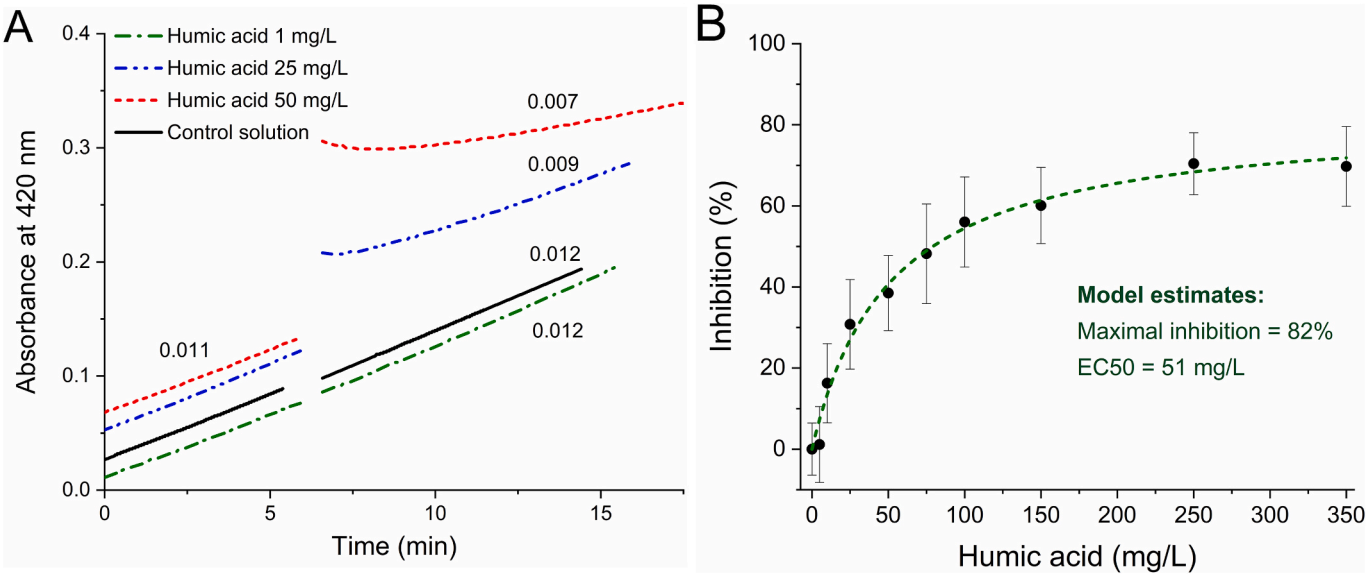

Fig. 3. Effect of humic acid on laccase-catalyzed oxidation of ABTS. (A) Assays of ABTS oxidation by laccase, in which small volumes of humic acid stock solution were added to the spectrophotometer cuvette to reach the final concentrations indicated. In the Control assay with the HA-blank solution (buffer without humic acid), a volume equivalent to the 50 mg/L humic acid was added to the cuvette. The oxidation rates in $\Delta Abs/\Delta t$ (min^{-1}) are indicated before and after the addition of humic acid (or Blank solution). (B) Inhibition of laccase-catalyzed oxidation of ABTS by humic acid. The inhibition was calculated from the oxidation rates in the presence of humic acid compared to the corresponding control rate in the absence of humic acid. The control oxidation rates in $\Delta Abs/\Delta t$ were 0.012 ± 0.003 min^{-1}. The line is the best non-linear regression fit of the data to eq. (1) in the text, and the corresponding parameters are indicated ($R^2 = 0.991$).

exhibits a significant affinity for binding hydrophobic and cationic species [19,20,27], which can be problematic for systems targeting hydrophobic pollutants like anthracene. At the assays' pH, MO is an anionic compound (pKa 3.45) and sequestration by HA is less probable. ABTS is a di-anionic substrate ($ABTS^{2-}$) of laccase in the acid media and even the product ABTS radical ($ABTS^{\bullet-}$) has a net negative charge [2].

When we evaluated the efficiency of the hexane extraction method employed in the laccase-catalyzed degradation of anthracene (described in the Methods Section 2.2), it was noted that high concentrations of HA could hinder the recovery of anthracene (at 1 mg/L) from aqueous media (Table S.1). However, recoveries close to 100 % were sustained with anthracene at a lower concentration, as those achieved in the reaction media after laccase incubations (approximately 0.3 mg/L), indicating that the HA interference with the hexane extraction is negligible concerning the final determination of anthracene degradation by the enzymatic system. Nevertheless, these results suggested that HA could indeed sequester and decrease the availability of anthracene in the conditions of the enzyme incubation assays, which could contribute to the lower efficiency of the laccase-ABTS system. The evaluation of the extraction efficiency was based on standards prepared in sodium acetate buffer, extracted and analyzed by HPLC as applied to the samples from enzymatic degradation assays, but without incubation. Therefore, two additional studies were put forward to assess the relevance of anthracene sequestration by HA.

Mimicking the enzymatic assays, anthracene at an initial concentration of 1 mg/L was incubated with different concentrations of HA, in the absence of enzyme or ABTS. The incubation lasted for 24 h, followed by extraction with hexane and HPLC analysis. Compared to parallel experiments without HA, the recovery of anthracene tended to decrease with increasing concentrations of HA, although significant effects were observed only with very high levels of HA (250 mg/L, Fig. S.4.A). Similar experiments were carried out with anthraquinone (Table S.1 and Fig. S.4.B), but even in the presence of the higher concentrations of HA no effect was detected. On this basis, the relevance of adsorption or covalent binding of anthraquinone to HA constituents in the conditions of the present work was discarded.

The interaction of anthracene and MO with HA was further evaluated by a different methodology, using HA entrapped in calcium alginate beads. This methodology (Methods Section 2.5) allowed to establish the interaction of anthracene with HA and, afterwards, quantify the adsorbate without the contact of the HA with the powerful extractant hexane. Anthracene and MO adsorption assays were carried out with calcium alginate beads containing HA, but also with unloaded beads, since alginate was described previously to adsorb some dyes and PAHs [27,41–43]. The assays were designed to test two adsorbent doses, corresponding to concentrations of HA 15 and 50 mg/L in the media. The results clearly indicated the adsorption of anthracene, both by unloaded and by HA-containing beads, but not of MO (Fig. 4). When the low adsorbent dose was used, the presence of 15 mg/L HA showed no significant effect on anthracene adsorption (Fig. 4.A). In the assays with the higher dose, a lower uptake capacity (mg per g of adsorbent) was measured, as expected, but 50 mg/L HA significantly increased the total amount of anthracene bound to the beads. However, it should be noted that the anthracene adsorbed to HA is only a small fraction, approximately 0.28 μg/mg of HA, so 50 mg/L HA could bind less than 0.02 mg/L of anthracene from solution, i.e. less than 20 % of the initially available anthracene. These results indicated that, at concentrations of 50 mg/L and higher, HA adsorbs anthracene under the conditions of the enzymatic assays. Still, it is unlikely that the small adsorption capacity of HA observed at 50 mg/L could inhibit 60 % anthracene degradation, as measured before (Fig. 1.B). Moreover, if HA sequestration of anthracene was the main mechanism limiting the efficiency of the laccase-ABTS system, it would be expectable that higher concentrations of HA (up to 500 mg/L in Fig. 1.B) would cause an escalating inhibition of anthracene transformation reaching 100 %, not the observed plateau of maximal inhibition at 70–80 %.

Regarding MO, no significant uptake was observed with any of the beads or doses (Fig. 4.B). In this case it is evident that sequestration of the substrate does not explains the HA inhibition of laccase, and the binding of the di-anionic ABTS to HA is even less plausible. So, other mechanisms of inhibition must justify the observed inhibition of the laccase catalytic systems.

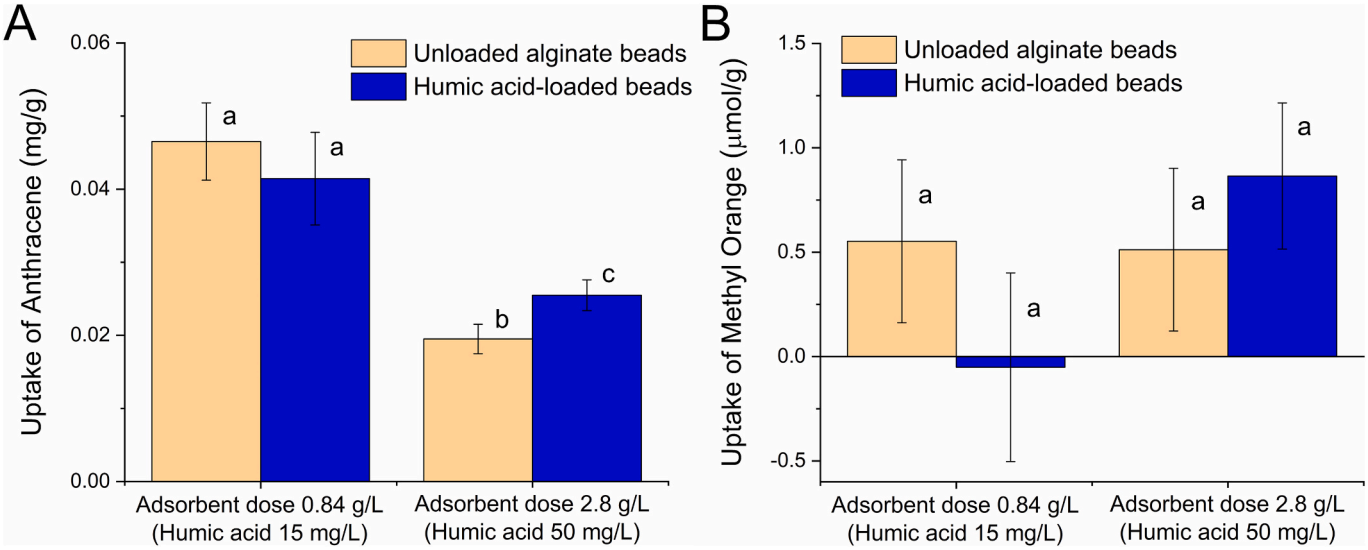

Fig. 4. Uptake of anthracene (A) and methyl orange (B) by alginate beads containing humic acid and by unloaded beads. Two amounts of each type of beads were tested corresponding to a dose of humic acid 15 and 50 mg/L in the media. After 48 h incubation, the bound anthracene was desorbed from the beads and measured by HPLC, while the removed methyl orange was calculated from the solution spectra. Different letters (a, b, c) indicate significant statistical differences ($p < 0.05$).

3.5. Scavenging of free radical reaction intermediates by humic acid

Laccase catalysis involves the generation of radical intermediates and products that might react with the HA co-present in the media [13,18]. This possible interference of HA with laccase systems was evaluated in the enzyme-catalyzed MO and ABTS oxidation reactional conditions (Figs. 5 and 6).

Following the assay of MO decolorization by laccase alone, as before, sodium azide was added after 30 min of catalysis, when a significant amount of MO degradation intermediates and products accumulated. As seen in Fig. 5, sodium azide blocked the enzyme and MO transformation. Then, HA was added to the reaction media to final concentrations of 75 or 150 mg/L. Apart from the initial increase with HA addition, the absorbance monitored for several minutes showed no changes, suggesting that HA does not reacts with any component of this reactional system detectable at the wavelength of the assay (Fig. 5). The laccase-catalyzed degradation of azo dyes, among other substrates, was proposed to proceed via phenoxy radicals and other reactive species [10,13,38], but the present results indicate that HA does not react with these intermediates.

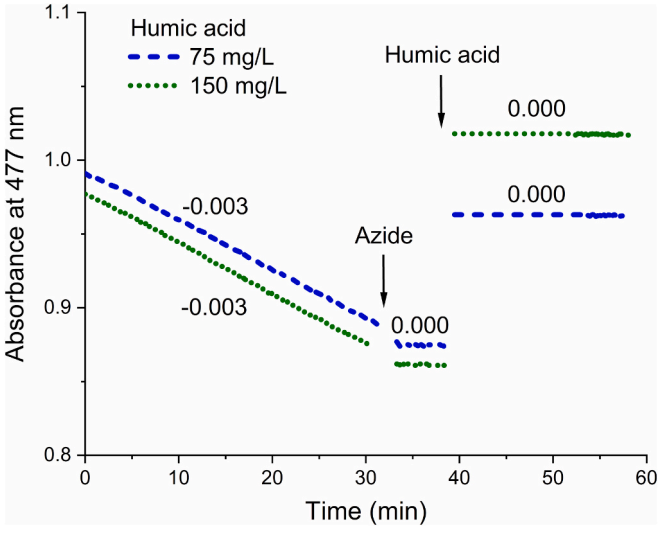

Fig. 5. Assays of humic acid addition to partially decolorized methyl orange. Firstly, methyl orange decolorization was catalyzed by laccase (alone) for 30 min and, then, the enzyme was blocked with sodium azide (0.2 mM). Shortly after stabilization of the absorbance, a small volume of humic acid stock solution was added to reach the indicated concentrations. Methyl orange was monitored at 477 nm and the observed ΔAbs/Δt (min^{-1}) are indicated for each reactional condition.

The ability of HA to react with the ABTS radical that is produced by laccase oxidation of ABTS was addressed by two methods: (1) interrupting laccase catalysis with azide as it was performed before with MO, and (2) using chemically (persulfate) produced ABTS radical. Fig. 6 shows a representative result obtained by the first approach. The laccase-catalyzed oxidation of ABTS progressed until a relevant concentration of the ABTS radical accumulated (absorbance approximately 0.5, equivalent to 14 μM), followed by enzyme blockage with azide. In these assays with a low concentration of laccase, 0.1 mM sodium azide was enough to fully inhibit the activity. After a few minutes for absorbance to stabilize, HA was added to the reaction media. As expected, a fast initial increase in absorbance was observed due to the HA addition, but then the absorbance clearly dropped with time. Control assays with the same stock solutions of enzyme and HA, but without sodium azide blocking, were carried out for comparison. As previously noted (Fig. 3. A), HA showed a biphasic effect on the evolution of the 420 nm absorbance also in this set of assays, being the first phase less perceptible when using lower concentrations of HA (Fig. 6.A). The presence of HA in the reaction mixture after laccase blockade, apart from the sudden initial increase, also showed a biphasic effect. In the first minutes, it caused a faster decline in the absorbance, obvious for example when using 150 mg/L of HA (Fig. 6.B), that gradually stabilizes to a lower decrease rate constant through several minutes.

Facing the important results with laccase-produced ABTS radical, we went on to confirm the reaction of HA with the radical also in an enzyme-free system. For these experiments, ABTS radical was produced by oxidating ABTS with persulfate, as described in Methods Section 2.6, and diluted in sodium acetate buffer for the HA tests similar to the previous assays with laccase. Representative results are given in Fig. S.5 of Supplementary Material and confirmed the ability of HA to decrease the absorbance of ABTS radical solutions. This effect can be explained by the probable antioxidant capacity of some constituents of HA to reduce the ABTS radical back to ABTS, causing the decline in the absorbance at 420 nm which is the characteristic maximum of an absorption band of the radical. The reducing constituents should have phenolic groups [18].

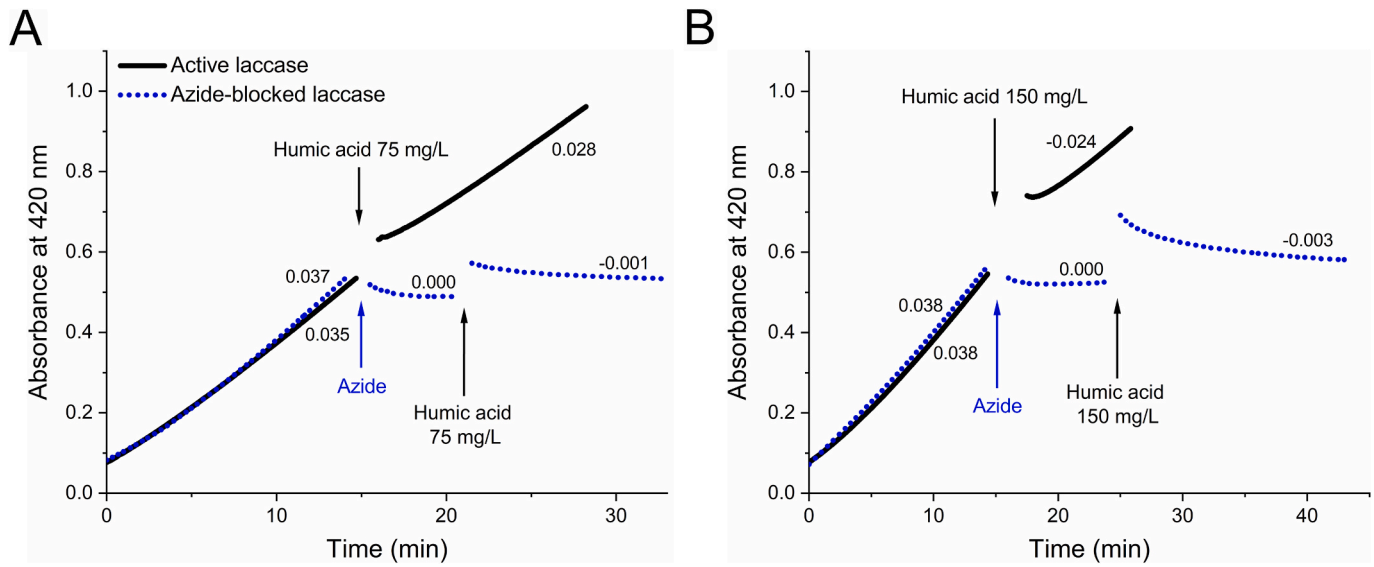

Fig. 6. Assays of the decay of ABTS radical on addition of (A) 75 mg/L and (B) 150 mg/L of humic acid. ABTS oxidation was catalyzed by laccase until absorbance came close to 0.5 and, then, the enzyme was blocked with sodium azide (0.1 mM) before addition of humic acid. An equivalent assay with non-inhibited enzyme is shown. ABTS radical was monitored at 420 nm and the observed ΔAbs/Δt (min^{-1}) are indicated for each reactional condition.

Some of the HA constituents with higher reducing potency and mobility might scavenge the radical faster, being responsible for the faster initial phase of absorbance drop. As these constituents are gradually consumed, the decrease decelerates and stabilizes in a low reduction rate maintained by constituents with lower potency but apparently abundant in the HA.

The ability of HA to scavenge ABTS radical will potentially interfere with the catalytic performance of all the laccase-ABTS systems, including those mediating anthracene and MO degradation studied before. Nonetheless, the comparison of the experimental traces like those shown in Fig. 6 indicated that radical scavenging does not completely accounts for the observed HA inhibition of ABTS oxidation by laccase. The fast initial effect of HA is difficult to compute precisely, but the steady rate of absorbance decrease (radical scavenging) maintained minutes after the HA addition was calculated as some thousandths of absorbance units per minute, indicated in Fig. 6. The inhibition of ABTS oxidation monitored by the effect on the absorbance change in the comparable control assays with active laccase was 4 to 9 times superior. When HA 75 mg/L was tested (Fig. 6A), radical scavenging was almost negligible, causing a stable rate of absorbance decrease of only −0.001. So, radical scavenging seems a relevant mechanism of interference with laccase-ABTS systems by HA at high concentrations, not for example at the EC_{50}s of inhibition of anthracene, MO and ABTS oxidation (Figs. 1.B, 2.B and 3.B).

3.6. Interaction of humic acid with copper ions of laccase

HA binds metal cations, showing a high affinity towards copper ions [19,20], so chelation of the laccase's copper ions responsible for the electron transfer between substrates can be hypothesized as a mechanism by which HA inhibits the enzyme activity. We investigated the relevance of the metal chelation mechanism by different approaches – molecular docking simulations and, experimentally, by making use of the laccase ABTS oxidation assay described in Methods Section 2.4.

The two models of *T. versicolor* laccase available at the Protein Data Bank (1gyc and 1kya) were used to simulate the docking of four models

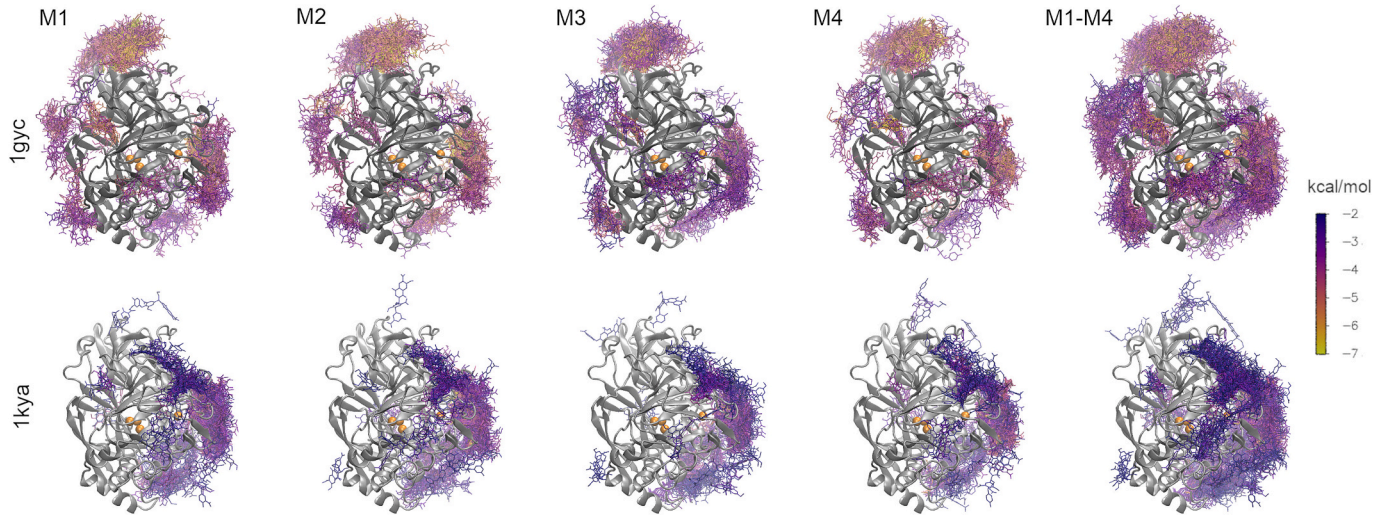

Fig. 7. Docking of four humic acid molecular models (M1 to M4) to two models of laccase, 1gyc (upper panel) and 1kya (lower panel). Laccase molecules are shown in gray and the copper ions as orange spheres. Humic acid poses are shown as sticks, colored by predicted binding energy, from violet (higher energy) to yellow (lower energy). Images M1 to M4 show the 500 poses for each humic acid model and M1-M4 overlays the poses for the four models (2000 poses).

of HA designated M1 to M4 (details in Methods Section 2.7). As depicted in Fig. 7, two main binding regions were found in 1gyc and three in 1kya laccase. When comparing the predicted binding energies (Fig. S.1.B), the protein model with better resolution - 1gyc - produced better docking poses both in terms of average and absolute values. Binding energies below −8 kcal/mol were estimated with this laccase model and the four HA models, but several poses were also predicted with energies around −6 kcal/mol with 1kya, which strongly suggests effective binding of the ligands to the enzyme. However, no poses were found with the HA models interacting directly with any of the laccase copper ions. The first binding region in 1gyc laccase harbors the poses with the lowest binding energies and encompasses the ends of some of the beta strands of the beta sandwich of domain 2 and the loops between strands (top region in Fig. 7; binding site residues listed in Fig. S.1.C), being far away from the copper ions. The other region in 1gyc is at the interface between domains 2 and 3 (right region in Fig. 7), and some poses of HA interact with histidine-458 that coordinates the single copper ion in this region (Fig. S.1.D). For the 1kya model, the region where more poses were found and with better binding energies corresponds to the second site of 1gyc described above, in the vicinity of the mononuclear T1 copper center.

The analysis of energy terms indicated that van der Waals interactions and hydrogen bonding (vdW + Hbond) contribute significantly more to the binding energy than electrostatic interactions, with both laccase models. The average vdW + Hbond and electrostatics energy terms for 1gyc were − 9.63 ± 1.92 kcal/mol and − 1.47 ± 0.77 kcal/mol, respectively. For 1kya, these values were − 9.81 ± 1.44 kcal/mol for vdW + Hbond and 0.08 ± 0.38 kcal/mol for electrostatics. When considering only the top 1 % best-scoring poses, the vdW + Hbond and electrostatics contributions for 1gyc are −14.76 ± 0.56 kcal/mol and − 1.51 ± 0.16 kcal/mol, respectively, while for 1kya, they are −13.78 ± 0.67 kcal/mol and − 0.14 ± 0.33 kcal/mol, respectively.

Experimentally, the susceptibility of the laccase copper centers was first addressed using DTPA, a strong metal chelator. As represented in Fig. 8.A, low concentrations of DTPA clearly inhibited the ABTS-oxidizing activity of laccase, indicating that the enzyme is sensitive to interference with the protein coppers. This is aligned with previous studies employing ethylenediaminetetraacetic acid (EDTA) and other metal chelators [2], including with the laccase from *T. versicolor* [24].

The experimental traces obtained in the assays, like those in Fig. 8.B, showed that DTPA promptly inhibits laccase on its addition to the reaction media, and does not exhibit the initial curvature observed with HA that results from the fast radical scavenging activity during the first minutes. Disregarding this initial curvature, the subsequent steady inhibition maintained by HA at 50 mg/L was identical to that caused by DTPA 0.4 mM, approximately 40 % (Fig. 8.B). Interestingly, when both DTPA and HA were added to laccase assays, a cumulative effect was observed, as shown in Fig. 8.B where sequential addition of the inhibitors caused approximately 80 % inhibition. These observations indicate that the two inhibitors have different mechanisms of action. Indeed, a clear difference in the inhibition profiles is that, contrary to HA (Fig. 3.B), DTPA can achieve complete inhibition of the enzyme (Fig. 8.A).

It is not clear if metal chelators inhibit laccase by simply interacting with the protein-bound coppers or actually remove the metals from the enzyme active site [2]. In some works, the laccases benefited from the addition of low concentrations of Cu^{2+} ions (typically up to 1 mM) that increased the enzymatic activity, suggesting that they were partially depleted of copper [2,15,22,24]. In the present study, supplementation of the reaction media with 1 mM $CuCl_2$ produced no significant effects and higher concentrations decreased laccase activity (Fig. S.6), in line with previous data [24] and the general assumption that laccases are isolated with the copper ions tightly bound [2].

Taking advantage that 1 mM Cu^{2+} ions had no influence on the activity, we decided to evaluate its effect on the HA-induced inhibition of laccase. If the inhibition by HA involves interaction with laccase metals, the supplementation of the reaction media with Cu^{2+} ions might occupy a part of the binding sites at HA and, by this way, lessen its inhibitory action. Strikingly, as shown in Fig. 9.A, the presence of 1 mM Cu^{2+} in the reaction media aggravated the inhibition of laccase observed after the addition of HA.

Additionally, in other assays with higher concentrations of HA and Cu^{2+} ions (not shown), it was possible to visually detect the formation of aggregates in the reaction media. It is well-known that metal cations, such as Cu^{2+} and Ca^{2+}, induce aggregation of HA [16], so we hypothesized that aggregation processes were influencing the observed inhibition of laccase. In this track, we tested the effect of Ca^{2+} ions on the HA-induced inhibition of laccase and the results were very similar to

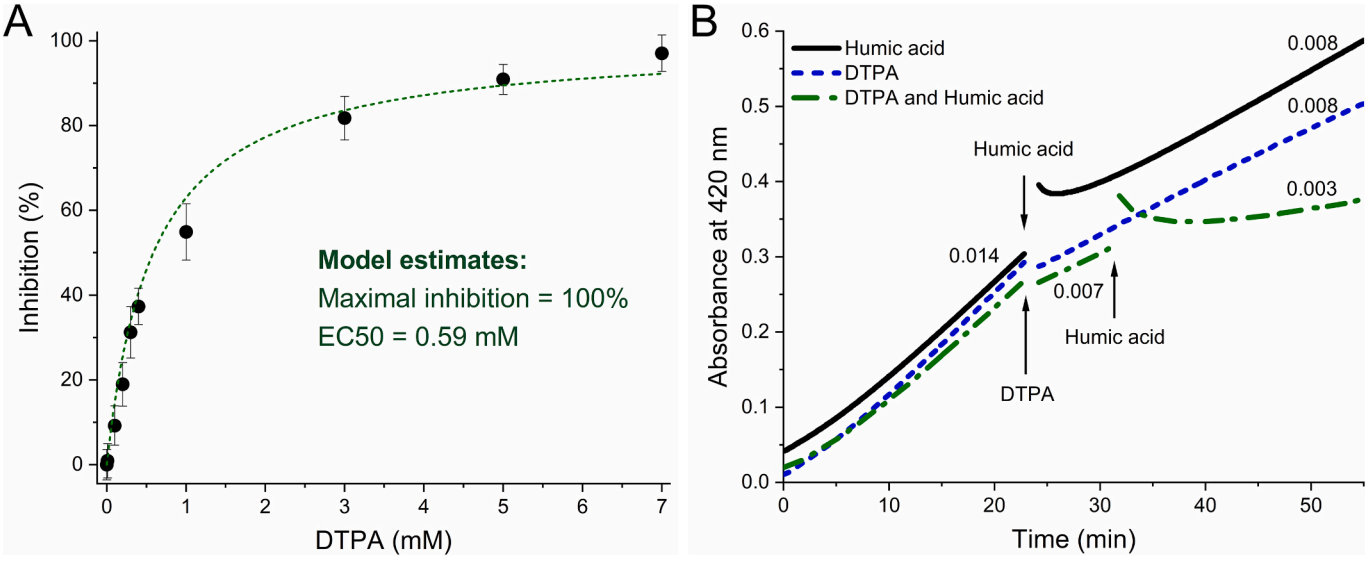

Fig. 8. Effect of diethylenetriaminepentaacetic acid (DTPA) on the ABTS-oxidizing activity and humic acid inhibition of laccase. (A) Inhibition of laccase-catalyzed oxidation of ABTS by DTPA. The inhibition was calculated from the oxidation rates in the presence of DTPA compared to the corresponding control rate in the absence of DTPA. The control oxidation rates in ΔAbs/Δt were 0.012 ± 0.001 min^{-1}. The line is the best non-linear regression fit of the data to the equation for a single-type binding site of DTPA in laccase, and the corresponding parameters are indicated ($R^2 = 0.971$). (B) Effect of DTPA (0.4 mM) on the humic acid (50 mg/L) inhibition of laccase. Oxidation rates in ΔAbs/Δt (min^{-1}) are indicated.

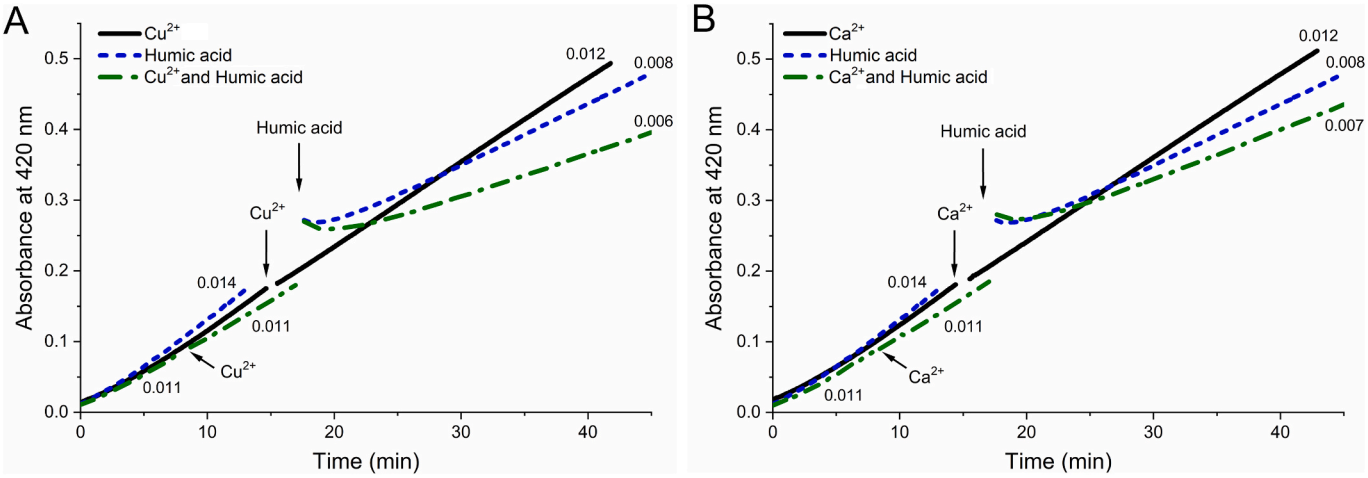

Fig. 9. Effect of (A) Cu^{2+} and (B) Ca^{2+} ions on the humic acid inhibition of laccase oxidation of ABTS. ABTS oxidation was monitored at 420 nm, and humic acid and/or metal ions were added to the spectrophotometer cuvette as depicted. The final concentrations of humic acid and metal ions were 50 mg/L and 1 mM, respectively. Oxidation rates in $\Delta Abs/\Delta t$ (min^{-1}) are indicated.

those observed with Cu^{2+} (Fig. 9.B). The Ca^{2+} ions also do not have any inhibitory effect on laccase up to 1 mM, so an indirect mechanism underlies the copper- and calcium-induced amplification of HA inhibition of laccase.

Overall, the results from the docking simulations and the experimental assays with DTPA and metal ions indicated that copper chelation is not a relevant mechanism of laccase inhibition by HA. Instead, the assays in media supplemented with Cu^{2+} and Ca^{2+} suggested the importance of aggregation phenomena in the HA action.

3.7. Aggregation of humic acid encapsulating laccase

In the presence of divalent cations, like Cu^{2+} and Ca^{2+}, HA forms intramolecular and intermolecular aggregates stabilized by charge

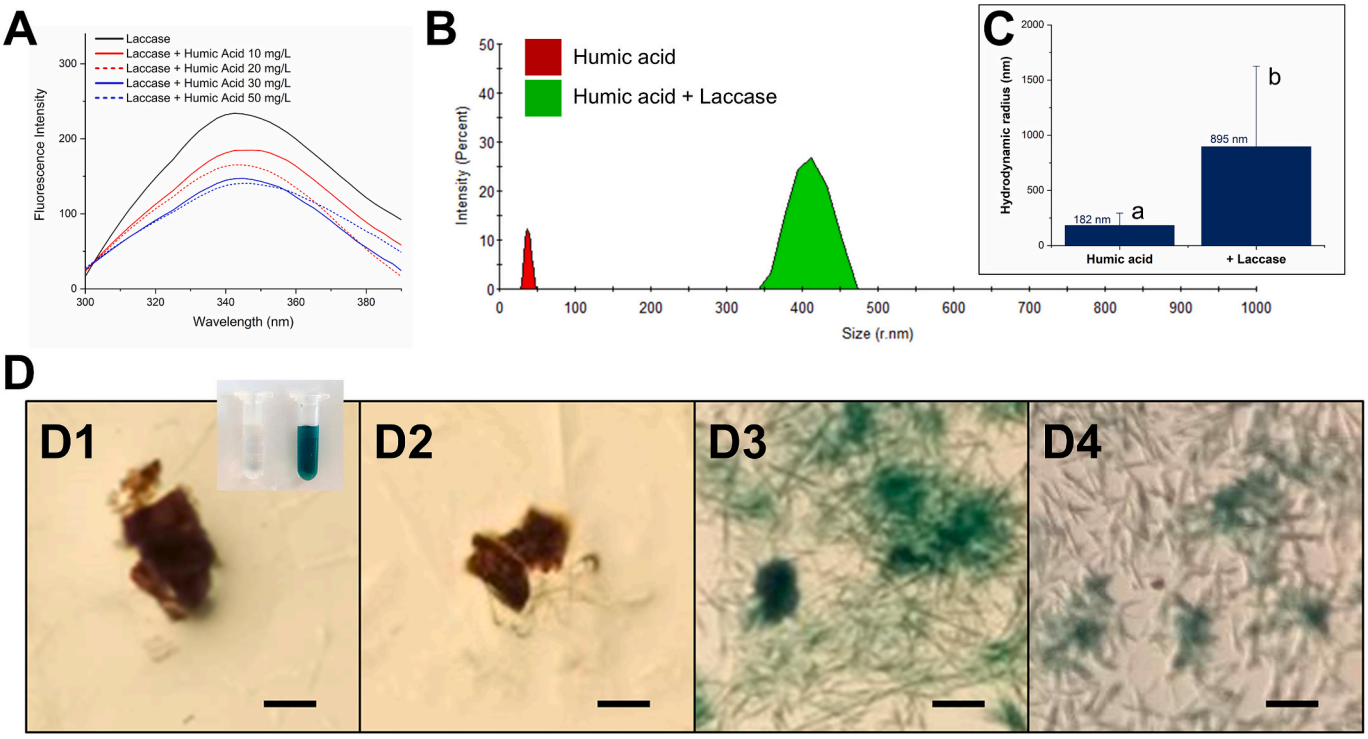

Fig. 10. Molecular interaction and aggregation of humic acid with laccase. The assays were carried out with laccase at a concentration of 20 μg/mL in pH 5 acetate buffer. (A) Changes in the fluorescence spectrum of laccase with increasing concentrations of humic acid. (B) Particle size distribution of aggregates of humic acid (20 mg/L) alone and after the addition of laccase, measured by dynamic light scattering. (C) Hydrodynamic radius of particles in humic acid 20 mg/L solutions before and after the addition of laccase. The mean values are indicated and the letters (a, b) indicate significant statistical difference ($p < 0.05$). (D) Microscopic observation of the aggregates of humic acid in the presence of calcium ions (D1 and D2), humic acid with laccase (D3) and humic acid with laccase in the presence of calcium ions (D4). Bar scales represent 10 μm. Calcium ions were used in D1, D2 and D4 at 1 mM. The ABTS substrate was added to all samples some minutes before observation, except D2. For the D2 sample, partially oxidized ABTS with bluish-green coloration was added instead of the fully reduced ABTS substrate of laccase. The inset in D1 shows microtubes with laccase without ABTS (left) and with ABTS incubated with laccase for several minutes developing the characteristic coloration of oxidized ABTS (right).

neutralization and functional group bridging [16]. The formation of complexes between HA and some proteins/enzymes, such as lysozyme, has also been described to give rise to flocs/aggregates that can reach micrometer size and shield the proteins [21,44–46]. Electrostatic attraction determines the complexation of HA with the net positively charged lysozyme, but the hydrophobic effect gives favorable contributions to the associations with trypsin and ribonuclease A, which have negative surface patches, and to the adsorption of Cry1Ab toxin to apolar HA [21,44,47]. In the case of urease, having a net negative charge at neutral pHs, hydrophobic attraction seems to prompt the interaction with HA, but causing only moderate changes in the structure of the enzyme [48]. Remarkably, the aggregation of the enzyme-HA complexes led to the encapsulation of the enzymes and suppression of the enzymatic activities [21,46], so we hypothesized that HA could inhibit laccase by forming complexes prone to aggregation that confines the enzyme.

We first probed the interaction of laccase with HA by the intrinsic fluorescence of the protein, a method recently employed with urease [48]. As shown in Fig. 10.A, the fluorescence spectra of laccase, with an excitation wavelength at 280 nm, presented a maximum emission at approximately 345 nm, in accordance with a fluorescence dominated by tryptophan residues. When HA was added to the enzyme, the fluorescence intensity gradually diminished with concentrations up to 30 mg/L, a strong indication of direct interaction of HA with laccase as predicted by the molecular docking simulations. Interestingly, the addition of higher concentrations of HA had no significant effect on the laccase fluorescence, resembling the plateaus observed before in the inhibition of the enzyme activities (Sections 3.2 and 3.3 of Results).

The formation of supramolecular aggregates was then investigated by DLS (Fig. 10.B and C). The assays were carried out with HA solutions at a concentration of 20 mg/L, in the range of the levels present in natural waters [16] and of the EC_{50} values calculated for the inhibition of the laccase catalytic systems described in previous sections. In these solutions with just HA, particles with hydrodynamic radii inferior to 230 nm were detected. This agrees with the coexistence of free monomers and small aggregates/soluble primary aggregates (sizes between 1 and 300 nm) described in other works on dilute HA solutions, namely at 30 mg/L and pH 5 [17,44]. When laccase was added to HA, a short 1-min equilibration period was enough for the formation of larger assemblies with hydrodynamic radii $\geq$350 nm (Fig. 10.B and C). The results from the fluorescence and DLS assays enabled to conclude that HA forms supramolecular complexes with laccase, even at a low concentration, and in a time scale matching the fast inhibition observed in the MO and ABTS oxidation assays.

Nevertheless, the flocculation/aggregation of enzyme-HA complexes could progress for up to 24 h (the incubation time in the anthracene degradation assays - Section 3.2). Being dependent on the conditions, typically 6 to 12 h were needed to visually perceive precipitation or microscopically observe the large micrometer aggregates of lysozyme-HA complexes at pH 5 [44–46,49]. In our reaction mixtures of diluted HA and laccase, macroscopic aggregates were not visually observed, except after 12–24 h if supplemented with Cu^{2+} or Ca^{2+} ions, suggesting that the laccase-HA aggregates are smaller than those with lysozyme and require the divalent ions to form large precipitating particles. However, by centrifuging the 24-h incubated mixtures to concentrate the particles, it became possible to observe microscopic aggregates that incorporate laccase (Fig. 10.D).

We optimized this methodology for microscopic inspection using solutions of HA and divalent ions. Maintaining HA at 20 mg/L, 24 h incubations in the presence of 1 mM Ca^{2+} promoted the formation of some aggregates visible under the microscope (Fig. 10.D1 and D2). Copper ions had a very strong effect and, at 3 mM, precipitating flocs were observed in the dilute HA solutions within some hours (results not shown). With the mixtures of HA and laccase, even without addition of divalent ions, aggregates with micrometer dimensions build-up (Fig. 10.D3), indicating that the laccase-HA complexes rapidly formed in short incubations (Fig. 10.B and C) keep aggregating through time. Applying the same methodology to solutions of laccase alone, no macro or microscopic particles were observed. Moreover, the microscopy method allowed to reveal the presence of laccase in the aggregates using the ABTS substrate. When ABTS was added to the aggregates before microscopic observation, the particles developed the bluish-green coloration typical of oxidized ABTS (Fig. 10.D3). The oxidation of ABTS was due to the enzyme, because the HA aggregates in the absence of laccase did not cause any colour change (Fig. 10.D1), and it was independent of the presence of Ca^{2+} (Fig. 10.D4). In a further control, considering the hypothesis that HA aggregates adsorb oxidized ABTS produced in solution, samples of HA (with Ca^{2+} ions) were incubated with pre-formed ABTS radical for the same time as the samples with the reduced ABTS, but the aggregates appeared with the coloration of plain HA aggregates (Fig. 10.D2).

4. Discussion

The results in this work give support to the detrimental interference of HA in the performance of laccase-based catalytic systems. In the four reactional systems studied, HA concentrations of environmental relevance caused a reduction in the measured conversion degree or rates. However, utmost 50 % inhibition can be expected with HA levels up to 20 mg/L in aqueous media, as observed with anthracene degradation by laccase-ABTS system. Our results are comparable to those reported for the transformation of 17β-estradiol by laccase alone [15] or of cyprodinil by the laccase-syringaldehyde system [7]. With laccase alone, HA at 30 mg/L caused inhibitions close to 50 %. In the second case, sizable inhibition was observed only with HA concentrations above 100 mg/L, and not even 400 mg/L blocked the catalyzed transformation.

An intriguing aspect observed in all reactional systems was that HA never reached 100 % inhibition of the enzyme, not even with very high concentrations (350 and 500 mg/L). Moreover, the substantial differences in the maximal inhibitions achieved and the EC_{50} values (from 5 to 51 mg/L) pointed out that HA interferes with the various laccase catalytic systems by different mechanisms.

The extraction and adsorption approaches employed herein converged on the ability of HA to decrease the availability of anthracene for laccase-catalyzed degradation, but only at high concentrations of HA (>50 mg/L). The extent of anthracene adsorption was negligible at HA levels around the EC_{50} of catalysis inhibition (21 mg/L) and, at higher concentrations, can only partially contribute to the observed interference with anthracene degradation. Our results showed that HA does not adsorb MO, consistent with the general understanding that HA binds mostly hydrophobic or positively charged molecules [19,20,27]. On this basis, adsorptive sequestration of anionic substrates or mediators like ABTS is also not probable.

An interesting ability of HA to reduce back the ABTS radical produced by laccase was firmly demonstrated in the present work. Electrochemical studies showed that humic substances contain phenolic electron-donating moieties with a wide range of redox potentials [18]. These moieties can act as antioxidants affecting pollutant oxidation reactions, for example by electron donation to oxidized intermediates. The kinetic assays revealed a biphasic behavior of HA, possibly due to the coexistence of HA components with different antioxidant reactivities. The ABTS radical scavenging activity of HA is potentially important especially because it will interfere with any laccase-ABTS system. Though, the rates of ABTS radical scavenging measured with different concentrations of HA are far from completely justifying the observed laccase inhibition. Moreover, the data obtained from MO assays and the ratio anthraquinone/anthracene give no support to HA interacting with the reaction intermediates or affecting the conversion paths in these reactional systems. It can be concluded that radical scavenging interferes with the laccase systems involving ABTS oxidation, but only partially and at HA concentrations above the EC_{50} values measured.

Another potential inhibition mechanism investigated was the HA

binding to the laccase's copper centers. Previous studies demonstrated that small metal chelators inhibit laccases from different sources [2], and mM concentrations of EDTA inhibited approximately 40 % the laccase extracted from *T. versicolor* [24]. Our data show for the first time that DTPA can inhibit 100 % of the enzyme activity, possibly due to stronger binding to the laccase's copper ions. DTPA is an amino-carboxilic acid-type metal chelating agent, like EDTA, but with a higher affinity for Cu^{2+} ions. The strength of the Cu^{2+}-DTPA complexes is expressed by the stability constant (log K) superior to 21, two orders of magnitude higher than the corresponding EDTA chelate [50]. Substantially inferior, the stability constant of Cu^{2+}-HA complexes was estimated between 10 and 11 [19]. Moreover, DTPA and HA showed a cumulative inhibition of laccase activity, and the HA inhibition was not prevented by supplementing the reaction media with divalent ions, all disapproving HA binding to the enzyme coppers. In agreement, the docking simulations suggested that HA can bind to laccase molecules at different regions, but even the T1 copper ion that is closer to the protein surface is not directly accessible to HA molecules. Worth noting, the molecular simulations predicted HA binding energies around −6 kcal/mol, which are comparable to those of well-established ligands like ABTS and guaiacol [51], and the interaction with a T1 copper-coordinating histidine can significantly influence the catalytic properties of the enzyme [52].The formation of aggregating laccase-HA complexes demonstrated herein provides a novel and general mechanism for understanding the interference of HA with laccase catalytic systems. The results showed that a 20 mg/L concentration of HA, as present in natural waters, allows interaction with laccase monitored by a decline in the fluorescence intensity of the protein. This HA concentration caused significant interference with the studied catalytic systems, hardly explainable by the conventional mechanisms of inhibition, namely the sequestration of substrates or target pollutants, the scavenging of reaction intermediates or the (completely discarded) chelation of coppers. In turn, the immobilization of the enzyme in complexes/aggregates with HA can suppress the laccase-based catalysis, as observed with other enzymes [21,46]. In addition to the possible inactivating denaturation of the protein, the immobilization and encapsulation of laccase restrains the mobility of the enzyme and mass transport of substrates/mediators/products of the reactions, hence decreasing the apparent turnover of the enzyme and the overall kinetics of the catalyzed reactions.

It is important to underline that the HA-induced decline of laccase fluorescence reaches a maximum after which higher concentrations of HA cause no further quenching of the fluorescence. This behavior is coherent with the observation of a maximum inhibition by HA, which remains clearly below 100 % across all the reactional systems studied in this work. The greater inhibitions achieved with higher concentrations of HA in the degradation of anthracene and in the ABTS oxidation reactions (approx. 80 %) can be justified by the sum of additional inhibitory mechanisms, namely, the anthracene sequestration and ABTS radical scavenging. Interestingly, it can also be argued that the immobilization of HA in the laccase-triggered aggregates equally limits its capacity to sequester anthracene molecules and to react with ABTS radicals, explaining why the HA does not impose a full inhibition of any of the enzymatic systems, in contrast to DTPA. The relevance of the encapsulation of the enzyme in the inhibition of the laccase-catalyzed reactions, over other mechanisms of HA inhibition, is especially reinforced by the results from the assays of MO decolorization by the laccase alone and mediator systems. Although these two systems are different catalytic processes, and indeed the mediator system shows a much faster kinetics, the HA inhibition curves are very similar, seemingly determined by the encapsulation of the enzyme and independent of the mediator's involvement or other specific characteristics of each process.

The comparison of four laccase-catalyzed reactional systems was a major strength of the present work, as well as the employment of complementary experimental techniques in the investigation of HA inhibitory mechanisms and laccase-HA aggregation. The data obtained by DLS and microscopy indicate that the laccase-HA complexes give rise to aggregates with heterogeneous sizes and that grow with time, hence difficult to predict with the current knowledge. However, the aggregates seem smaller than the quite large lysozyme-HA assemblies that present macroscopic aggregation/flocculation [44–46,49]. It can be speculated that HA interaction with laccase is comparable to that described with urease [48], but further studies are warranted on the molecular details of the complexes and the properties of the formed aggregates. Another present limitation that should be addressed in future work is the potential impact of water and wastewater constituents, such as iron ions and small organic molecules, on HA inhibition of laccase.

CRediT authorship contribution statement

João Lopes: Methodology, Investigation. **Dorinda Marques-da-Silva:** Validation, Methodology. **Cláudia Peralta:** Methodology, Investigation. **Joaquim Rui Rodrigues:** Writing – review & editing, Methodology, Investigation. **Daniela Vaz:** Writing – original draft, Supervision, Methodology. **Ricardo Lagoa:** Writing – review & editing, Writing – original draft, Supervision, Methodology, Conceptualization.

Funding

This research was funded by Fundação para a Ciência e Tecnologia (FCT—Portugal) through the project PTDC/BIA-MIB/31864/2017 and the PhD scholarship reference 2023.04204.BD awarded to J.L.. It was also supported by national funds through FCT/MCTES (PIDDAC) to the research units: LSRE-LCM, UIDB/50020/2020 (DOI: 10.54499/UIDB/50020/2020) and UIDP/50020/2020 (DOI: 10.54499/UIDP/50020/2020); ALiCE, LA/P/0045/2020 (DOI: 10.54499/LA/P/0045/2020); and CQC, UIDB/00313/2020 (DOI: 10.54499/UIDB/00313/2020).

Declaration of competing interest

The authors declare that they have no known competing financial interests or personal relationships that could have appeared to influence the work reported in this manuscript.

Appendix A. Supplementary data

Supplementary data to this article can be found online at https://doi.org/10.1016/j.ijbiomac.2025.146405.

Data availability

Data will be made available on request.

References

[1] S. Riva, Laccases: blue enzymes for green chemistry, Trends Biotechnol. 24 (5) (2006) 219–226, https://doi.org/10.1016/j.tibtech.2006.03.006.
[2] J.M. Lopes, D. Marques-da-Silva, P.Q. Videira, R.L. Lagoa, Comparison of laccases and hemeproteins systems in bioremediation of organic pollutants, Curr. Protein Pept. Sci. 23 (6) (2022) 402–423, https://doi.org/10.2174/1389203723666220704090416.
[3] Z. Chen, K. Du, F. Li, et al., Mussel-inspired laccase-mediated polydopamine graft onto bamboo fibers and its improvement effect on poly(3-hydroxybutyrate) based biocomposite, Int. J. Biol. Macromol. 238 (March) (2023) 123985, https://doi.org/10.1016/j.ijbiomac.2023.123985.
[4] A.I. Yaropolov, O.V. Skorobogat'ko, S.S. Vartanov, S.D. Varfolomeyev, Laccase, Appl. Biochem. Biotechnol. 49 (3) (1994) 257–280, https://doi.org/10.1007/BF02783061.
[5] K. Piontek, M. Antorini, T. Choinowski, Crystal structure of a laccase from the fungus Trametes versicolor at 1.90-Å resolution containing a full complement of coppers, J. Biol. Chem. 277 (40) (2002) 37663–37669, https://doi.org/10.1074/jbc.M204571200.
[6] J. Lopes, D. Marques-da-Silva, P.A. Videira, A.K. Samhan-Arias, R. Lagoa, Cardiolipin membranes promote cytochrome c transformation of polycyclic aromatic hydrocarbons and their in vivo metabolites, Molecules 29 (5) (2024) 1129, https://doi.org/10.3390/molecules29051129.

[7] K.H. Kang, J. Dec, H. Park, J.M. Bollag, Transformation of the fungicide cyprodinil by a laccase of Trametes villosa in the presence of phenolic mediators and humic acid, Water Res. 36 (19) (2002) 4907–4915, https://doi.org/10.1016/S0043-1354(02)00198-7.
[8] A. Arca-Ramos, G. Eibes, G. Feijoo, J.M. Lema, M.T. Moreira, Coupling extraction and enzyme catalysis for the removal of anthracene present in polluted soils, Biochem. Eng. J. 93 (2015) 289–293, https://doi.org/10.1016/j.bej.2014.10.015.
[9] B.L.B. Perini, R.L. Bitencourt, N.A. Daronch, A.L. dos Santos Schneider, D. de Oliveira, Surfactant-enhanced in-situ enzymatic oxidation: A bioremediation strategy for oxidation of polycyclic aromatic hydrocarbons in contaminated soils and aquifers, J. Environ. Chem. Eng. 8 (4) (2020) 104013, https://doi.org/10.1016/j.jece.2020.104013.
[10] L.D. Ardila-Leal, R.A. Poutou-Piñales, A.M. Pedroza-Rodríguez, B.E. Quevedo-Hidalgo, A brief history of colour, the environmental impact of synthetic dyes and removal by using laccases, Molecules 26 (13) (2021) 3813, https://doi.org/10.3390/molecules26133813.
[11] J.M. Sarkar, J.M. Bollag, Inhibitory effect of humic and fulvic acids on oxidoreductases as measured by the coupling of 2,4-dichlorophenol to humic substances, Sci. Total Environ. 62 (1987) 367–377, https://doi.org/10.1016/0048-9697(87)90524-9.
[12] A. Siripornprasarn, E. Luepromchai, M.A. Nanny, Mechanisms by Which Soluble Humic Substances Alter the Kinetics of Pentachlorophenol Transformation by Trametes versicolor Laccase, Environ. Eng. Sci. 28 (11) (2011) 819–825, https://doi.org/10.1089/ees.2010.0485.
[13] W. Jiang, W. Li, F. Xiao, D. Wang, Z. Wang, Influence of NOM and SS on the BPA removal via peroxidase catalyzed reactions: Kinetics and pathways, Sep. Purif. Technol. 173 (2017) 244–249, https://doi.org/10.1016/j.seppur.2016.09.029.
[14] Y. Yang, J. Li, H. Shi, L. Zhai, X. Wang, S. Gao, Influence of natural organic matter on horseradish peroxidase-mediated removal of 17α-ethinylestradiol: role of molecular weight, J. Hazard. Mater. 356 (December 2017) (2018) 9–16, https://doi.org/10.1016/j.jhazmat.2018.05.032.
[15] Q. Yang, W. Dong, Z. Ye, et al., Effect of environmental factors on laccase-mediated 17β-estradiol coupling reaction, Sci. Rep. 15 (1) (2025) 14765, https://doi.org/10.1038/s41598-025-98586-9.
[16] A. Rodrigues, A. Brito, P. Janknecht, M.F. Proença, R. Nogueira, Quantification of humic acids in surface water: effects of divalent cations, pH, and filtration, J. Environ. Monit. 11 (2) (2009) 377–382, https://doi.org/10.1039/B811942B.
[17] M.J. Avena, K.J. Wilkinson, Disaggregation Kinetics of a Peat Humic Acid: Mechanism and pH Effects, Environ. Sci. Technol. 36 (23) (2002) 5100–5105, https://doi.org/10.1021/es025582u.
[18] M. Aeschbacher, C. Graf, P. Schwarzenbach R, Sander M., Antioxidant Proprieties of Humic Acid, Environ. Sci. Technol. 46 (2012) 4916–4925.
[19] A. Prado, J. Torres, P. Martins, J. Pertusatti, L. Bolzon, E. Faria, Studies on copper (II)- and zinc(II)-mixed ligand complexes of humic acid, J. Hazard. Mater. 136 (3) (2006) 585–588, https://doi.org/10.1016/j.jhazmat.2005.12.035.
[20] J. Xu, L.K. Koopal, L. Fang, J. Xiong, W. Tan, Proton and Copper Binding to Humic Acids Analyzed by XAFS Spectroscopy and Isothermal Titration Calorimetry, Environ. Sci. Technol. 52 (7) (2018) 4099–4107, https://doi.org/10.1021/acs.est.7b06281.
[21] J.E. Tomaszewski, R.P. Schwarzenbach, M. Sander, Protein Encapsulation by Humic Substances, Environ. Sci. Technol. 45 (14) (2011) 6003–6010, https://doi.org/10.1021/es200663h.
[22] O. Saoudi, N. Ghaouar, Biocatalytic characterization of free and immobilized laccase from Trametes versicolor in its activation zone, Int. J. Biol. Macromol. 128 (2019) 681–691, https://doi.org/10.1016/j.ijbiomac.2019.01.199.
[23] F.J. Enguita, D. Marçal, L.O. Martins, et al., Substrate and Dioxygen Binding to the Endospore Coat Laccase from Bacillus subtilis, J. Biol. Chem. 279 (22) (2004) 23472–23476, https://doi.org/10.1074/jbc.M314000200.
[24] M. Lorenzo, D. Moldes, S. Rodríguez Couto, M.A. Sanromán, Inhibition of laccase activity from Trametes versicolor by heavy metals and organic compounds, Chemosphere 60 (8) (2005) 1124–1128, https://doi.org/10.1016/j.chemosphere.2004.12.051.
[25] J. Li, Y. Zhang, J. Peng, X. Wu, S. Gao, L. Mao, The effect of dissolved organic matter on soybean peroxidase-mediated removal of triclosan in water, Chemosphere 172 (2017) 399–407, https://doi.org/10.1016/j.chemosphere.2017.01.013.
[26] R. Re, N. Pellegrini, A. Proteggente, A. Pannala, M. Yang, C. Rice-Evans, Antioxidant activity applying an improved ABTS radical cation decolorization assay, Free Radic. Biol. Med. 26 (9–10) (1999) 1231–1237.
[27] D. Marques-da-Silva, J.M. Lopes, I. Correia, J.S. Silva, R. Lagoa, Removal of hydrophobic organic pollutants and copper by alginate-based and polycaprolactone materials, Processes 10 (11) (2022) 2300, https://doi.org/10.3390/pr10112300.
[28] R.M.P. Silva, J.P.H. Manso, J.R.C. Rodrigues, R.J.L. Lagoa, A comparative study of alginate beads and an ion-exchange resin for the removal of heavy metals from a metal plating effluent, J. Environ. Sci. Health A 43 (11) (2008) 1311–1317, https://doi.org/10.1080/10934520802177953.
[29] G.M. Morris, R. Huey, W. Lindstrom, et al., AutoDock4 and AutoDockTools4: Automated docking with selective receptor flexibility, J. Comput. Chem. 30 (16) (2009) 2785–2791, https://doi.org/10.1002/jcc.21256.
[30] T. Bertrand, C. Jolivalt, P. Briozzo, et al., Crystal structure of a four-copper laccase complexed with an arylamine: Insights into substrate recognition and correlation with kinetics, Biochemistry 41 (23) (2002) 7325–7333, https://doi.org/10.1021/bi0201318.
[31] J. Mikuni, N. Morohoshi, Cloning and sequencing of a second laccase gene from the white-rot fungus Coriolus versicolor, FEMS Microbiol. Lett. 155 (1) (1997) 79–84, https://doi.org/10.1111/j.1574-6968.1997.tb12689.x.
[32] E.C. Meng, T.D. Goddard, E.F. Pettersen, et al., UCSF ChimeraX: Tools for structure building and analysis, Protein Sci. 32 (11) (2023), https://doi.org/10.1002/pro.4792.
[33] J.M. Word, S.C. Lovell, J.S. Richardson, D.C. Richardson, Asparagine and glutamine: using hydrogen atom contacts in the choice of side-chain amide orientation, J. Mol. Biol. 285 (4) (1999) 1735–1747, https://doi.org/10.1006/jmbi.1998.2401.
[34] C. Niederer, K.U. Goss, Quantum Chemical Modeling of Humic Acid/Air Equilibrium Partitioning of Organic Vapors, Environ. Sci. Technol. 41 (10) (2007) 3646–3652, https://doi.org/10.1021/es062501b.
[35] N.D. Corona-Motolinia, B. Martínez-Valencia, L. Noriega, et al., Synthesis, crystal structure, and computational methods of vanadium and copper compounds as potential drugs for cancer treatment, Molecules 25 (20) (2020) 4679, https://doi.org/10.3390/molecules25204679.
[36] W. Humphrey, A. Dalke, K. Schulten, VMD: Visual molecular dynamics, J. Mol. Graph. 14 (1) (1996) 33–38, https://doi.org/10.1016/0263-7855(96)00018-5.
[37] R. Huey, G.M. Morris, A.J. Olson, D.S. Goodsell, A semiempirical free energy force field with charge-based desolvation, J. Comput. Chem. 28 (6) (2007) 1145–1152, https://doi.org/10.1002/jcc.20634.
[38] M. Chhabra, S. Mishra, T.R. Sreekrishnan, Immobilized laccase mediated dye decolorization and transformation pathway of azo dye acid red 27, J. Environ. Health Sci. Eng. 13 (1) (2015) 38, https://doi.org/10.1186/s40201-015-0192-0.
[39] H. Forootanfar, S. Rezaei, H. Zeinvand-Lorestani, et al., Studies on the laccase-mediated decolorization, kinetic, and microtoxicity of some synthetic azo dyes, J. Environ. Health Sci. Eng. 14 (1) (2016) 7, https://doi.org/10.1186/s40201-016-0248-9.
[40] Cajthaml T. Eibes, M.T. Moreira, G. Feijoo, J.M. Lema, Enzymatic degradation of anthracene, dibenzothiophene and pyrene by manganese peroxidase in media containing acetone, Chemosphere 64 (3) (2006) 408–414, https://doi.org/10.1016/j.chemosphere.2005.11.075.
[41] R. Shokoohi, Z. Torkshavand, M.M. Mahmoudi, A.M. Behgoo, E. Ghaedrahmati, F. M. Hosseini, Effective removal of azo dye reactive blue 222 from aqueous solutions using modified magnetic nanoparticles with sodium alginate/hydrogen peroxide, Environ. Prog. Sustain. Energy 38 (s1) (2019) S205–S213, https://doi.org/10.1002/ep.12971.
[42] A. Mokeddem, S. Benykhlef, A.A. Bendaoudi, et al., Sodium alginate-based composite films for effective removal of Congo red and Coralene Dark Red 2B dyes: kinetic, isotherm and thermodynamic analysis, Water 15 (9) (2023) 1709, https://doi.org/10.3390/w15091709.
[43] T. Song, W. Tian, J. Zhao, K. Qiao, M. Zou, M. Chu, N-doped reduced graphene oxide nanocomposites encapsulated sodium alginate/polyvinyl alcohol microspheres for anthracene and its oxygenated-PAH removal in aqueous solution, J. Taiwan Inst. Chem. Eng. 125 (2021) 168–175, https://doi.org/10.1016/j.jtice.2021.06.016.
[44] W.F. Tan, L.K. Koopal, W. Norde, Interaction between humic acid and lysozyme, studied by dynamic light scattering and isothermal titration calorimetry, Environ. Sci. Technol. 43 (3) (2009) 591–596, https://doi.org/10.1021/es802387u.
[45] W.F. Tan, L.K. Koopal, L.P. Weng, W.H. van Riemsdijk, W. Norde, Humic acid protein complexation, Geochim. Cosmochim. Acta 72 (8) (2008) 2090–2099, https://doi.org/10.1016/j.gca.2008.02.009.
[46] Y. Li, W. Tan, L.K. Koopal, M. Wang, F. Liu, W. Norde, Influence of soil humic and fulvic acid on the activity and stability of lysozyme and urease, Environ. Sci. Technol. 47 (10) (2013) 5050–5056, https://doi.org/10.1021/es3053027.
[47] J.E. Tomaszewski, M. Madliger, J.A. Pedersen, R.P. Schwarzenbach, M. Sander, Adsorption of insecticidal Cry1Ab protein to humic substances. 2. influence of humic and fulvic acid charge and polarity characteristics, Environ. Sci. Technol. 46 (18) (2012) 9932–9940, https://doi.org/10.1021/es302248u.
[48] Y. Li, L.K. Koopal, Y. Chai, et al., Spectroscopic investigation of conformational changes in urease caused by interaction with humic acid, Colloids Surf. B Biointerfaces 215 (April) (2022) 112510, https://doi.org/10.1016/j.colsurfb.2022.112510.
[49] W.K.W.A. Khodir, A. Hakim, M. Kobayashi, Strength of flocs formed by the complexation of lysozyme with leonardite humic acid, Polymers (Basel). 12 (8) (2020) 14–16, https://doi.org/10.3390/polym12081770.
[50] J.R. Hart, Ethylenediaminetetraacetic acid and related chelating agents, in: Ullmann's Encyclopedia of Industrial Chemistry vol. 13, 2011, pp. 573–578, https://doi.org/10.1002/14356007.a10_095.pub2.
[51] K. Agrawal, J. Shankar, P. Verma, Multicopper oxidase (MCO) laccase from *Stropharia* sp. ITCC-8422: an apparent authentication using integrated experimental and in silico analysis, 3 Biotech 10 (9) (2020) 413, https://doi.org/10.1007/s13205-020-02399-8.
[52] F. Vianello, G. Miotto, M.T. Cambria, G.P.P. Lima, P. Vanzani, M.L. Di Paolo, Kinetic role of a histidine residue in the T1 copper site of the laccase from *Rigidoporus lignosus*, J. Mol. Catal. B Enzym. 99 (2014) 34–42, https://doi.org/10.1016/j.molcatb.2013.10.017.